Turun yliopisto
University of Turku

FIELD-EFFECT BASED CHEMICAL AND BIOLOGICAL SENSING: THEORY AND IMPLEMENTATION

Matti Kaisti

TURUN YLIOPISTON JULKAISUJA – ANNALES UNIVERSITATIS TURKUENSIS
Sarja - ser. A I osa - tom. 552 | Astronomica - Chemica - Physica - Mathematica | Turku 2017

University of Turku

Faculty of Mathematics and Natural Sciences

Department of Future Technologies

Supervised by

Ari Paasio
Department of Future Technologies
University of Turku
Joukahaisenkatu 3 20520 Turku
Finland

Kalle Levon
Department of Chemical and Biomolecular Engineering
New York University
Brooklyn NY 11201
USA

Tero Soukka
Department of Biochemistry
University of Turku
Tykistökatu 6 A 20520 Turku
Finland

Reviewed by

Edwin Chihchuan Kan
Electrical and Computer Engineering
Cornell University
Ithaca, New York 14853
USA

Jukka Lekkala
Department of Automation Science and Engineering
Tampere University of Technology
P.O. Box 692, FI-33101 Tampere
Finland

Opponent

Ioannis (John) Kymissis
Department of Electrical Engineering
Columbia University
500 W120th Street, New York, NY 10027
USA

ISBN 978-951-29-6712-4 (PRINT)

ISBN 978-951-29-6713-1 (PDF)

ISSN 0082-7002 (Print)

ISSN 2343-3175 (Online)

Painosalama Oy - Turku, Finland 2017

Abstract

Electrochemical sensors share many properties of an ideal (bio)chemical sensor. They can be easily miniaturized with high parallel sensing capabilities, with rugged structure and at low cost. The response obtained from the target analyte is directly in electrical form allowing convenient data post-processing and simple interfacing to standard electrical components. With field-effect transistor (FET) based sensors, the transducing principle relies on direct detection of interfacial charge allowing detection of various ions and charged macromolecules.

This thesis investigates FET based sensors for biological and chemical sensing. First, an ion-sensitive floating gate FET (ISFGFET) structure is studied and modeled. The proposed model reveals novel abilities of the structure not found in conventional ion-sensitive FETs (ISFETs). With ISFGFET, we can simultaneously optimize the transistor operating point and modulate the charging of the surface and the ionic screening layer via the field effect. This control is predicted to allow reduced electric double layer screening as well as the possibility to enhance charged molecule attachment to the sensing surface. The model can predict sensor characteristic curves in pH sensing in absolute terms and allows any potential to be computed in the sensor including the electrical part and the electrolyte solution. Furthermore, a compact ISFGFET variant is merged into electric circuit simulator, which allows it to be simulated as a standard electrical component with electrical simulations tools of high computational efficiency, and allows simple modifications such as addition of parasitic elements, temperature effects, or even temporal drifts.

Next, another transistor based configuration, the extended-gate ISFET is studied. The simplicity of the proposed configuration allows a universal potentiometric approach where a wide variety of chemical and biological sensors can be constructed. The design philosophy for this sensing structure is to use the shelf electric components and standard electric manufacturing processes. Such an extended-gate structure is beneficial since the dry electronics can be completely separated from the wet sensing environment. The extended-gate allows simple functionalization towards chemical and biological sensing. A proof-of-concept of this structure was verified through organo

modified gold platforms with ion-selective membranes. A comparison with standard open-circuit potentiometry reveals that the sensing elements in a disposable sensing platform arrays provide comparable performance to traditional electrodes. Finally, a universal battery operated hand-held electrical readout device is designed for multiplexed detection of the disposable sensors with wireless smartphone data plotting, control, and storage.

Organic polymers play an important role in the interfacial properties of sensors studied in this thesis. The polymer coating is attractive in chemical sensing because of its redox sensitivity, bio-immobilization capability, ion-to-electron transducing capability, and applicability, for example via a simple low-cost drop-casting. This structure simplifies the design of the sensor substantially and the coating increases the amount of possible target applications.

Tiivistelmä

Elektrokemiallisilla sensoreilla on monta ideaalisen (bio)kemiallisen sensorin ominaisuutta. Ne soveltuvat hyvin miniatyrisointiin sekä usean elementin yhtäaikaiseen mittaamiseen. Lisäksi tekniikka mahdollistaa kestävän rakenteen alhaiseen hintaan. Sensorin ulostulo on suoraan sähköisessä muodossa, joka mahdollistaa kätevän datan jälkikäsittelyn ja yksinkertaisen integroinnin olemassa oleviin elektronisiin komponentteihin. Yksi merkittävä elektrokemiallinen sensoriluokka perustuu kanavatransistoreihin, jotka mittaavat hilalla tapahtuvaa sähkövarauksen muutosta. Näiden sensorien avulla on mahdollista mitata mm. varauksellisia ioneja ja makromolekyylejä.

Tässä työssä tutkitaan transistoreihin perustuvia (bio)kemiallisia sensoreita. Ensiksi tutkittiin sekä mallinnettiin uuden tyyppistä ioni-selektiivistä kanavatransistorisensoria, jossa on kelluva hila. Rakennetun mallin avulla löydettiin uusia ominaisuuksia, jotka eivät ole perinteisillä rakenteilla mahdollisia. Uudella rakenteella on mahdollista optimoida transistorin toimintapiste, mutta tämän lisäki myös voidaan kontrolloida elektrolyyttiliuoksen yli vaikuttavaa sähkökenttää. Menetelmä mahdollistanee herkemmän ja nopeamman biologisten makromolekyylien mittaamisen. Mallin avulla sensorin pH-vaste voidaan määrittää absoluuttisesti ja tämän lisäksi mikä tahansa potentiaali tai varaus systeemin eri pisteissä voidaan laskea. Lisäksi kehitetty malli integroitiin osaksi elektroniikan piirisimulaattoria. Tämä mahdollistaa sensorin simuloinnin osana laajempia kokonaisuuksia sekä parasiittisten efektien tehokkaan mallintamisen.

Seuraavaksi kehitettiin toinen transistoripohjainen rakenne. Tavoitteena oli luoda yksinkertainen rakenne, jonka avulla on mahdollista tehdä monia erityyppisiä potentiometrisiä sensoreita. Suunnitteluperiaatteena oli hyödyntää olemassa olevia komponentteja ja valmistusprosesseja. Lisäksi rakenne hyödyntää transistorin hilan jatkamisen niin, että elektroninen osa on kokonaan ilmassa ja ainoastaan detektoiva pinta on nesteessä. Tämä poistaa käytännössä kokonaan yleisesti tunnetun kotelointiongelman. Lisäksi rakenne tarjoaa erittäin kustannustehokkaan ratkaisun kertakäyttöisiin sovellutuksiin. Kyseinen hilarakenne on myös helppo funktionalisoida tavoitesovellutuksesta riippuen. Sensorirakenne verifioitiin funktionalisoimalla se orgaanisella polymeerillä sekä ioni-selektiivisellä membraanilla. Sensoria ver-

rattiin perinteiseen potentiometriin. Rakenne tarjoaa yhtä hyvää tai osittain parempaa suorituskykyä verratuna perinteisempiin ratkaisuihin. Lopuksi kehitettiin patterikäyttöinen laite, jonka avulla voidaan mitata yhtäaikaisesti useampaa sensorielementtiä kehitetyssä kertakäyttöisessä alustassa. Mittauksen ohjaus, tallennus sekä havainnointi tehdään älypuhelimen avulla.

Orgaaniset polymeerit vaikuttavat merkittävästi tutkittujen sensoreiden ominaisuuksiin. Kyseisillä polymeereillä on monia hyödyllisiä ominasuuksia kuten redox-herkkyys, mahdollisuus immibilisoida biomolekyylejä, ioni-elektronikonversio sekä mahdollisuus yksinkertaiseen funktionalisointiin. Esitetty rakenne yksinkertaistaa sensorin suunnittelua merkittävästi ja polymeerin avulla tehty funktionalisointi laajentaa sovellutusmahdollisuuksia huomattavasti.

Acknowledgements

The research in this thesis is based on the work carried out in the Technology Research Center (now Department of Future Technologies) at the University of Turku during 2014 - 2016. I am thankful for the Jenny and Antti Wihuri Foundation for funding the bulk of my research as well as Tekniikan edistämissäätiö for the financial support.

Foremost I would like to thank my supervisors for the opportunity to work in a field of electrochemistry to which I had no previous exposure and for their support in starting new research here in the University of Turku. Prof. Ari Paasio was always very flexible when arranging practicals matters. I thank Prof. Tero Soukka for his enthusiastic support as well as educating and introducing me to the science of molecular diagnostics. Prof. Kalle Levon provided the initial seed for this research and he has been an integral part throughout this project.

This thesis would not have been possible without the collaboration of my colleagues. I was lucky enough to meet Dr. Zhanna Boeva, polymer chemist who was able to withstand educating an engineer without any background in chemistry. I believe it suffices to say that without her dedication in science and collaborative efforts my thesis would not be even close to ready at this point and would most likely look quite different. Also, I wish to thank the personnel in Åbo Academi who were always very welcoming and friendly.

Dr. Ari Lehmusvuori has been a strong collaborator during this journey and together we have worked towards new nucleic acid sensors. Ari is a strong-minded scientist with the ability to commit and move forward even the most difficult tasks at hand.

Tero Koivisto and Dr. Mikko Pänkäälä allowed a smooth start to the project by helping in the early steps. In addition I thank Dr. Teijo Lehtonen for helping me with my first and successful funding proposal.

The first experiments would not have been possible without the open mindedness of Prof. Carita Kvarnström and Dr. Pia Damlin. The first experimental work was carried out with their support.

Dr. Qi Zhang has been a close collaborator throughout this project. Although there is smallish pond between Turku and New York we have shared many discussions and ideas and helped each other in science domains

unfamiliar to us otherwise.

I had the privilege to work together with many students in various topics during this project. Aapo Knuutila was the first student involved and the one whom with we made the first experiments. Juho Koskinen and Sami Nieminen made great contributions when we implemented the electrical design into a working device as final work package of this project. These efforts saved a considerable time and we were able to work together very efficiently and created a robustly working device with minimal debugging. In addition I thank the lab personnel Peter Virta and Mika Taskinen for their help in creating the first data logger. This work was also supported by Tapani Talvitie, a close friend since the days at the Turku University of Applied sciences where we competed for the superiority in electronics. He showed great friendship by helping with the electronics design during the thesis. It also became clear why others are called students and others professionals.

I was privileged to get two great pre-examiners to work on my thesis. Prof. Jukka Lekkala did a superb job with many broad as well as detailed suggestions on how to improve the thesis. I thank Jukka for the great contribution and for the significant time he put into the review. Prof. Edwin Kan is greatly acknowledged for his time and effort in examining my thesis. Edwin, as one the leading experts in the field, gave indispensable guidance and points to think about concerning the field. I am most grateful for Prof. Ioannis (John) Kymissis for his willingness to make a long travel from New York to Turku and honored to have him as the opponent. John has been most flexible and supportive throughout the arrangements and he deserves my warmest thanks.

Although the road needs to be traveled alone it would not have been possible without the help and support of my family. My mom, Risto and Kaija were always supportive and understanding on the tolls of the project and more than often took care of my own children and allowed me to concentrate of getting the work done.

Last, I want to dedicate this work to the rest of my team members: Toivo, Hertta and Aino.

List of original publications

I Q. Zhang, H. S. Majumdar, M. Kaisti, A. Prabhu, A. Ivaska, R. Österbacka, A. Rahman, and K. Levon. Surface functionalization of ion-sensitive foating-gate field-effect transistors with organic electronics. *IEEE Transactions on Electron Devices*, 62(4):1291-1298, 2015. [122]

II M. Kaisti, Q. Zhang, A. Prabhu, A. Lehmusvuori, A. Rahman, and K. Levon. An ion-sensitive oating gate fet model: Operating principles and electrouidic gating. *IEEE Transactions on Electron Devices*, 62(8):2628-2635, 2015. [63]

III M. Kaisti, Q. Zhang, K. Levon. Compact Model and Design Considerations of an Ion-Sensitive Floating Gate FET. *Sensors and Actuators B: Chemical*, 241(31), 2016 [65]

IV M. Kaisti, A. Knuutila, Z. Boeva, C. Kvarnström, and K. Levon. Low-cost chemical sensing platform with organic polymer functionalization. *IEEE Electron Device Letters*, 36(8):844-846, 2015. [64]

V M. Kaisti, Z. Boeva, J. Koskinen, S. Nieminen, J. Bobacka, K. Levon. Hand-held Transistor based electrical and multiplexed chemical sensing system. *ACS Sensors*, 2016 [66]

Contributions of the author:

I Participated in the model derivation and device behavior explanation, analyzing the data and writing the manuscript.

II Conceived the idea, developed the model, analyzed the data and wrote the manuscript.

III Conceived the idea, developed the model, analyzed the data and wrote the manuscript.

IV Conceived the idea, designed the sensing platform, planned the experiments, analyzed the data, developed the measurement setup and wrote the manuscript. The experiments were done jointly with one of the co-authors.

V Conceived the idea, designed the sensing platform as well as the electronics and the mechanics of the read-out device, wrote the manuscript and managed the project. The planning of the experiments, experimental work and the data analysis were done jointly with one of the co-authors.

Symbols and Abbreviations

β_{int}	Buffering capacity
α	Sensitivity coefficient
χ_{sol}	Constant dipole potential
ϵ_0	Vacuum permittivity
ϵ_r	Dielectric constant
ϵ_w	Dielectric constant of an electrolyte solution
λ_D	Debye screening length
ϕ_f	Fermi potential of the semiconductor
ϕ_{Si}	Silicon work function
Ψ_0	Sensing surface potential
Ψ_{DL}	Potential at the Stern layer
σ_0	Surface charge density
σ_{DL}	Double layer surface charge density
σ_{SG}	Sensing gate charge density
a_i	Activity of species i
c_0	Ion concentration
C_{CG}	Control gate capacitance
C_{DL}	Double layer capacitance
C_{Gouy}	Diffuse layer capacitance
C_{OX}	Channel gate oxide capacitance
C_{SG}	Sensing gate capacitance
C_{Stern}	Stern capacitance
e	Elementary charge

E_{ref}	Constant interfacial potential of the reference electrode
E_{SG}	SG electric field strength
F	Faraday constant
I_D	Drain current
k	Boltzmann constant
$K_{A,B}$	Dissociation constant
$K_{i,j}$	Selectivity coefficient
L	Limit of detection coefficient
n_0	Bulk ion number density
N_A	Avogadro constant
N_S	Total number of binding sites per unit area
pH_B	Bulk electrolyte solution pH
pH_{PZC}	pH of zero charge
Q_0	Initial trapped charge in the FG
Q_i	Charge induced at the floating gate
Q_{tot}	Total semiconductor charge density
R	Gas constant
T	Temperature
V_{CG}	Control gate potential
V_{FG}	Floating gate potential
V_{REF}	Reference electrode potential
z	Valence of an ion
ADC	Analog to digital converter
Al_2O_3	Aluminium oxide
CG	Control gate
ChemFET	Chemically sensitive field-effect transistor
CMOS	Complementary metal oxide semiconductor
CVCC	Constant-voltage-constant-current
DAC	Digital to analog converter
DNNSA	Dinonylnaphtalenesulfonic acid

DNNSA	Dinonylnaphthalene sulfonic acid
DOS	Dioctyl sebacate
EDL	Electric double layer
EG-ISFET	Extended-gate ISFET
EnFET	Enzyme field-effect transistor
ENIG	Electroless nickel immersion gold
FG	Floating gate
FGFET	Floating gate field-effect transistor
GC	Glassy carbon
GCS	Gouy Chapman Stern
GEMSS	General electric multiplexed sensing system
HRP	Horseradish peroxidase
ISE	Ion-selective electrode
ISFET	Ion-selective field-effect-transistor
ISFGFET	Ion-sensitive floating gate field-effect transistor
ISM	Ion-selective membrane
KTFPB	potassium tetrakis [3,5-bis(trifluoromethyl) phenyl] borate
MOSFET	Metal-oxide-semiconductor field-effect transistor
OCP	Open-circuit-potential
PANI	Polyaniline
PCB	Printed-circuit-board
PCR	Polymerase chain reaction
PDMS	Polydimethylsiloxane
PEI	Polyethyleneimine
POC	Point-of-care
PVC	Polyvinylchloride
PZC	Point of zero charge
RIE	Reactive-ion etching
SEM	Scanning electron microscopy
SG	Sensing gate

Si_3N_4	Silicon nitride
SiNW-FET	Silicon nanowire field-effect transistor
SiO_2	Silicon dioxide
SPICE	Simulation program with integrated circuit emphasis
V_{cell}	Electrochemical cell potential
V_{th}^{isfet}	ISFET threshold voltage
V_{th}^{mosfet}	MOSFET threshold voltage

Contents

Chapter 1

Introduction

The global biosensor market is estimated to grow to USD 22.5 billion industry in 2020 with 9.7 percent annual growth from 2014 [33]. The significant growth in the biosensor market can be attributed to increasing demand of point-of-care (POC) tests. Chronic and lifestyle associated diseases, aging population, and the increasing number of applications for biosensing in different industries are all driving the market growth. Similarly, the global environmental monitoring market is expected to have annual growth of 7.5 percent and reach a market value of USD 20.5 billion in 2020. Global population control, policies aimed to reduce pollution, and increased funding towards such aims are seen as factors pushing the growth of the market in the Asia-Pacific region. [26]

In POC sensing, the most common target is glucose. Diabetes mellitus requires frequent testing of blood glucose levels and it affects more than 125 million people worldwide. Glucose meters account about 85 percent of global biosensing markets.[37]. Other common targets in POC sensing include cholesterol, triglycerides, creatinine, lactate, ammonia, urea and ionic blood chemicals, such as H^+, Na^+ and K^+. [37]. Immunoassays have also matured for POC tests and the most well known is the home pregnancy test detecting the hormone human chorionic gonadotropin (hCG); other examples of commercial tests are for testing HIV, Influenza AB and group A Streptococcus.[37] Nucleid acid diagnostics are also emerging, e.g., BioFire Diagnostics (acquired by bioMerieux in 2014) and Cepheid GeneXpert have recently released a gastrointestinal panel.

The use of electrochemical sensors is promising for creating truly portable sensors of low-cost, solid-state nature, and ruggedness with simple data handling on a large scale. These methods provide a broad spectrum of different analytes to be tested such as nucleic acids, proteins, enzymatic reactions, ions, and metabolites. The common electrochemical sensors can be categorized into potentiometric, amperometric, and impedimetric sensors. [54]

Amperometric sensors obtain information from the concentration-current relationship by measuring the current flowing through the cell. Impedimetric sensors detect the changes in either the capacitance or resistance between electrodes when a varying sinusoidal signal is fed to the electrochemical cell. Potentiometric sensors have a capacitive input and are zero-current sensors that detect the electrochemical potential between two electrodes. A notable success story among the electrochemical sensors can be found in the amperometric glucose meter [37].

Among various potentiometric techniques, the ion-selective field-effect transistor (ISFET) has attracted considerable attention because of its potential for small size, low weight, fast response time, ruggedness, low output impedance, and the capability of direct on-chip integration with sensor array configurations for multiplexed detection and electrical readout as well as suitability for mass production for portable systems. [21, 100, 93] The concept of an ISFET was introduced in the early 1970s. It was realized that a MOSFET with the metal gate removed and the underlying gate oxide inserted in an aqueous solution along with a reference electrode was responsive to ions and notably to pH. Due to the importance of hydrogen ion, most early publications concentrated on its detection including experimental and modeling efforts.[11] The gate of the FET can be modified for detection of other ions using suitable selective membranes [54] or for detection of biomolecular interactions via biological recognition elements [100] [93] The recognition element determines the sensor specificity towards a certain chemical species. The recognition layer can be in some cases be directly coupled to the FET gate or an additional transducing layer can be incorporated. The obtained information is the concentration/activity of the target analyte or the presence of a biomolecule. As a final step, the signal can be amplified, processed, displayed [100] or sent to the cloud [88] depending on the application. The components of a general FET based (bio)chemical sensor are illustrated in Fig 1.1.

Figure 1.2 shows the number of publications [1] with historical landmarks during the past four decades showing a clear acceleration in the number of published papers after the turn of millennia. From the invention of the ISFET in 1970, the development first concentrated on the detection of inorganic ions using selective membranes already developed for conventional ion-selective-electrodes [54]. The first enzyme FET was realized by Janata and Caras in 1980 [19] for the direct detection of penicillin and the concept of an immunoFET was described in 1978 [59]. The first label-free detection of complementary DNA probe-target hybrization was achieved in 1997 by Souteyrand et al. [105] The first sensor arrays compatible with commer-

[1] Scopus with search string (sensor AND FET) OR (biosensor AND FET) OR ISFET, 13.4.2016

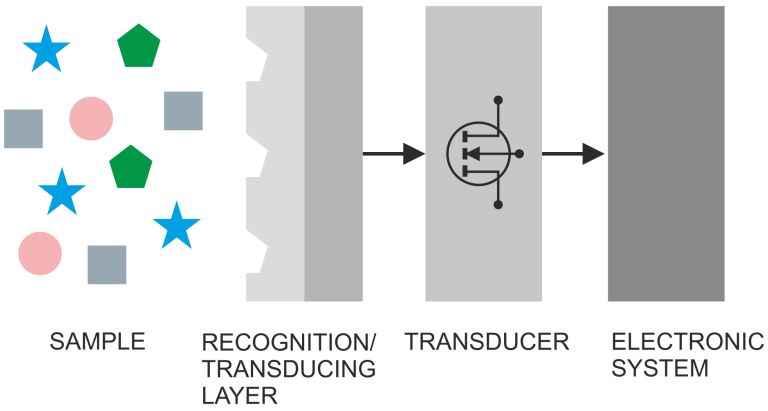

Figure 1.1: Illustration of a (bio)chemical sensor.

cial CMOS processes were described in the same year with pH-ISFETs in a 15x16 array. [119] In some of the more recent efforts, the focus has shifted from detecting various targets to new nanoFET structures, namely silicon nanowire FETs (SiNW-FET) first described in 2001 [22] and graphene based field-effect sensors for DNA detection. [81] A notable achievement was published in 2010 when transistor based genome sequencing was demonstrated by the Ion Torrent, ThermoFisher Scentific. [98] Interestingly the technology is based on the well known and studied hydrogen ion sensing at the ISFET gate and the floating-gate CMOS array, where the main idea is to use massively parallel detection and piggy back the well developed semiconductor industry. During the incorporation of a nucleotide in the common construction of the secondary strand from the template, a hydrogen ion is released. This creates a time variant detectable change in pH near the sensing surface. [98, 111]

Despite significant efforts, the progress towards commercial miniaturized and multiplexed devices has been modest. Encapsulation of electronics from the wet environment has created significant difficulties in creating robust and mass producible sensors. In laboratory settings, such encapsulations have been demonstrated successfully on numerous occasions, but applicability for mass production, especially if aqueous storage medium is required remains unclear. [45]

Regardless, research efforts show no sign of diminishing. New directions in the field are concentrating on new highly sensitive nanoscale devices and novel materials [121, 126] to enhance responses and reach lower detection limits, portable and miniature designs, and highly integrated sensor circuits. [83, 85]

It is noteworthy to point that most biosensor concepts are only demonstrated in buffer conditions rather than in real samples. [45]. The prepa-

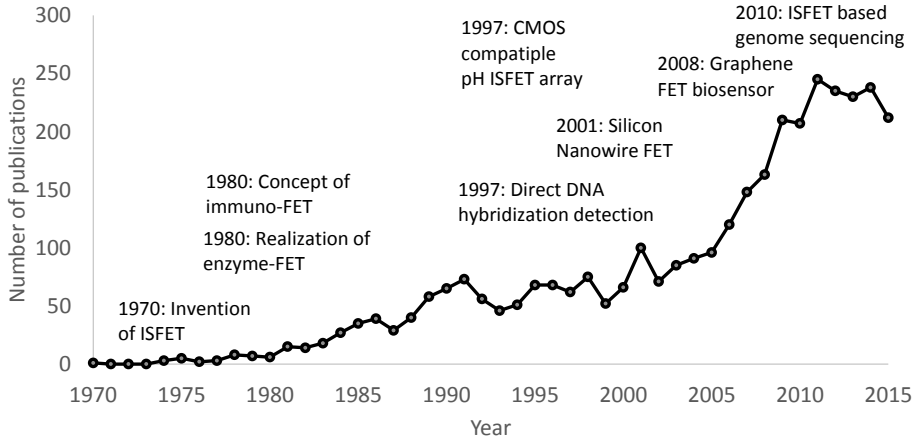

Figure 1.2: Number of publication of transistor based (bio)chemical sensors with technological landmarks.

ration in real samples is a step required in most biosensing applications. Additionally, novel detection schemes claiming extremely low detection limits have been challenged.[21, 107]. When ISFETs are reduced in size for nanoscale devices, it has been argued that particularly in low sample concentrations the amount of time it takes for a biomolecule to bind the surface will be impractically long with a time scale of days. Moreover, a strong critique toward the community developing biosensors claims that there is a lack of understanding of principal concepts and that experimental results are mostly artifacts [53]. Moreover, the sensitivity is usually considered as the figure of merit above all other sensor characteristics such as reliability. Further, it is usual to check device operation only in buffers with minimal selectivity tests. [45]

This thesis focuses on two different FET based detection schemes. Although in both cases the electrolyte/solid physics is the same, the structures have quite different behavior. The first and more intriguing sensor structure utilizes an additional control gate, allowing simultaneous control of the FET operating point as well the charging conditions of the fluid. This structure is expected to be beneficial in a broad spectrum of applications as it might be possible to use it for charged molecule control via the field effect. [60, 28, 58] Here we study such a device and develop a model that predicts device behavior, and we verify it through experiments.

The second structure is simpler in construction and has a lesser degree of freedom in detection, but provides a low cost and robust alternative. Substantial effort is done to create a fully miniaturized system comprising a disposable low cost sensing platform that interfaces to miniaturized wireless

read out electronics using commercial components and fabrications processes only. Such a system provides a platform that should help to bridge the gap between FET based sensor development and chemical research concerning interfacial properties.

This thesis is organized as follows: Chapter 2 reviews the literature and introduces the basic sensing concepts relevant to the work that follows. Chapter three describes the aims of the original publications 3. The used materials and methods are summarized in Chapter 4. Chapter 5 summarizes the results with discussions before conclusions in chapter 6.

Chapter 2

Literature Review

Ion sensitive field-effect transistors (ISFETs) were introduced in the 1970s by Bergveld [9] and have since received significant attention. The first commercial application was a pH meter [11] and more recently the Ion Torrent technology utilizes massively parallel CMOS arrays with pH sensitive ISFETs for next generation sequencing and competes with more established optical systems.[98] In POC testing, Quantum MDx is anticipating to launch its hand-held SiNW-FET based Q-POC device in 2016 [1].

At the moment, pH-ISFET probes are sold commercially by several companies [i.e., Thermo Fisher Scientific (USA), Sentron (Netherland), Microsens S.A. (Switzerland), Honeywell (USA), D + T Microelectronica (Spain)]. These sensors are mostly intended for general laboratory purposes and thus they have sizes and designs similar to traditional ion-selective electrodes, although needle-type probes for specific applications mainly in the food industry, for meat, beverages, and even for direct soil monitoring are available. Companies providing analytical instrumentations based on ISFETs outsource the device fabrication to few foundries specialized in non-standard microelectronic fabrication processes. [62]

The variety of different field-effect sensor structures is vast and the amount of sensing materials and different measured target analytes provides an incredible number of different sensor system combinations. Here, the focus is on different transistor structures and on the interfacial behavior at the electrolyte/solid interface. We emphasize that existing manufacturing processes with new device structures such as SiNW-FETs and graphene FETs are mostly still in the device development phase and are not matured as robust mass fabricated sensors. For recent reviews not in the scope of the present work the reader is referred to [94] for a broad electrochemical sensors review, [91] for biosensors in general, [3] for CMOS based sensing, [79] for label free detection, and [117] for electrochemical immunosensors for point

[1] http://www.quantumdx.com/ 23.5.2016

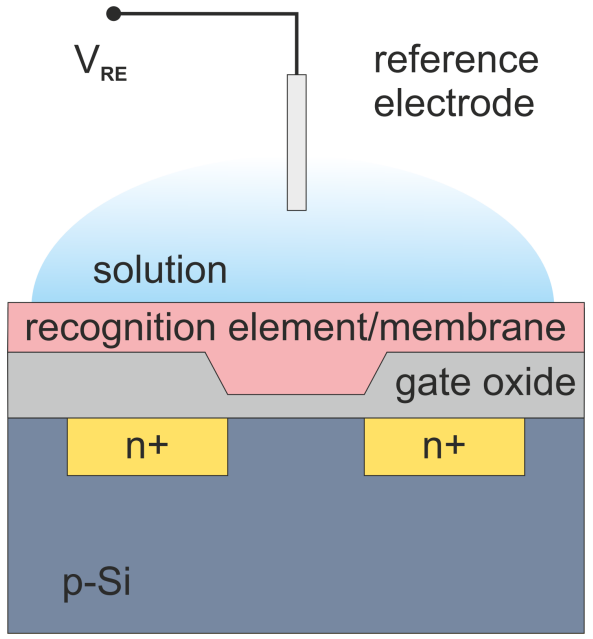

Figure 2.1: Illustration of an ion-sensitive field-effect transistor (ISFET)

of care diagnostics.

2.1 Working Principle of Field-Effect Sensors

2.1.1 Ion-sensitive Field-effect Transistor (ISFET)

The ISFET is a potentiometric device that operates in a similar way to a metal oxide semiconductor field-effect transistor (MOSFET). The basic structure of an ISFET resembles that of an MOSFET and is illustrated in Figure 2.1. The gate of the MOSFET is removed and the underlying gate oxide is exposed and placed in direct contact with an electrolyte solution. When the gate is immersed in an electrolyte solution, a double layer is formed at the interface. The potential drop, Ψ_0 across the double layer is determined by the surface charge density σ_0 as well as the double layer capacitance C_{DL} as $\Psi_0 = \sigma_0/C_{DL}$. [10, 39] Ionic composition, surface charging due to analyte concentration changes, as well as biological recognition events lead to changes in σ_0 and C_{DL} and the changes in them are usually monitored as changes in threshold voltage V_{th} or the drain current I_D.

ISFET operation is best described through the MOSFET. The structure of both are similar. [11] The voltage at the gate oxide through the field effect accumulates charge carriers to the channel. A threshold voltage is defined as the voltage required at the gate to create a strong inversion at the

channel, i.e., a conducting channel is formed via inversion rather than doping. [109] The channel and its conductivity can then be controlled via the gate voltage. In ISFETs, the potential is applied through the reference electrode to bias the transistor in its conductive state and subsequent changes in the surface charge of the sensing membrane creates a voltage shift affecting the conductance of the transistor.

The most commonly used oxide sensing membranes are SiO_2, Si_3N_4, Al_2O_3 and Ta_2O_5. Such devices have inherent sensitivity towards hydrogen ion due to the oxide's amphotheric hydroxyl groups that can either protonate or depronotonate in response to changes of the solution pH. [39] The detection is based on a change in surface charge, which creates a potential difference across the solution referred against the reference electrode immersed into the solution. This modulates the transistor channel conductance and subsequently the drain current. The FET is set to an operating point through a reference electrode that sets the bulk solution potential in contact with the sensing membrane. With a large enough potential, the transistor channel starts conducting. This leads the drain current to depend on the drain-source voltage and channel conductance, which can be controlled by the reference electrode as well as by varying the chemical potential at the interface.

There are many different variants of ISFET electrical structures and sensing materials as well as methods for their fabrication. Despite the vast variety of structures, however, all of them are basically charge sensing devices and the detection is based on a varying electric field that modulates the transistor channel conductance. In the many different implementations, the basic principles remain the same and are commonly described through the ISFET threshold voltage.

In the case of MOSFET, the threshold voltage is related to the material properties. The ISFET threshold voltage is a modified MOSFET threshold voltage and reads [10]

$$V_{th}^{isfet} = E_{ref} - \Psi_0 + \chi_{sol} - \frac{\Phi_{Si}}{e} - \frac{Q_{tot}}{C_{ox}} + 2\phi_f \tag{2.1}$$

where E_{ref} is a constant interfacial potential related to the reference electrode. The interfacial potential of the electrolyte/oxide interface consists of a constant dipole potential χ_{sol} and a pH depended surface potential Ψ_0. The typical MOSFET parameters are the silicon work function ϕ_{Si}, the total semiconductor charge density Q_{tot} , the oxide capacitance per unit area C_{ox}, the Fermi potential of the semiconductor ϕ_f, and the electron charge e.

In modern ISFET structures, the MOSFET gate is not removed leading to slight modifications to the above MOSFET related expressions. Additionally, this creates an added series capacitor as the gate oxide is no longer directly the sensing membrane, but it is capacitively coupled via a connecting

metal to the passivation layer of a CMOS chip acting as a sensing membrane. However, the fundamental principle is the same and a simplified expression of the ISFET V_{th} can be given as [104] [31]

$$V_{th}^{isfet} = V_{th}^{mosfet} + V_{chem} \tag{2.2}$$

where V_{chem} lumps all the chemically related parameters

$$V_{chem} = E_{ref} - \Psi_0 + \chi_{sol} - \frac{\phi_m}{q} \tag{2.3}$$

and also be presented with a modified Nernst equation

$$V_{chem} = \gamma - 2.3\frac{kT}{q}\alpha pH \tag{2.4}$$

where the γ is a constant that lumps all constant chemical potentials for simplified expression, α is a sensitivity coefficient ranging from 0 to 1 describing the deviation from the ideal Nernstian responses, and k,T are the Boltzmann constant and the absolute temperature respectively. [31]

These sensors can be functionalized with other materials to be sensitive to other ions, called chemically sensitive FETs (ChemFETs), or by modifying the surface with biologically active media leading to BioFETs. [100]

2.1.2 Coated Wire

In the early 1970s, an analoguous technique to ISFET was developed by Cattrall and Freiser called the coated wire electrodes [20]. Conventional ion-selective electrodes (ISE) require internal filling solutions and an ion-selective membrane. In the coated wire arrangement, a metal wire is directly coated with an ion-selective membrane. This allows the construction of a much simpler, smaller, inexpensive and robust sensor compared to conventional ISE.

Despite its attractive properties, it was soon realized that the construction exhibited stability issues because of high interfacial charge-transfer resistance at the substrate/membrane interface. [54]. The mismatch between the conduction mechanisms of the ionically conductive membrane and the electrically conductive substrate blocks the flow of charge at the interface. This results in an unstable potential. To create a stable interfacial potential, reversible electrode processes at the interface are required. This can be achieved with an additional intermediate layer having mixed ionic and electronic conductivity. [113] [14]. Such an intermediate layer is commonly referred as a solid contact.

Figure 2.2 illustrates a typical cell using all solid state electrodes with solid contacts. The potentiometric cell is typically constructed using two electrodes, a reference electrode and a working electrode to which a solid

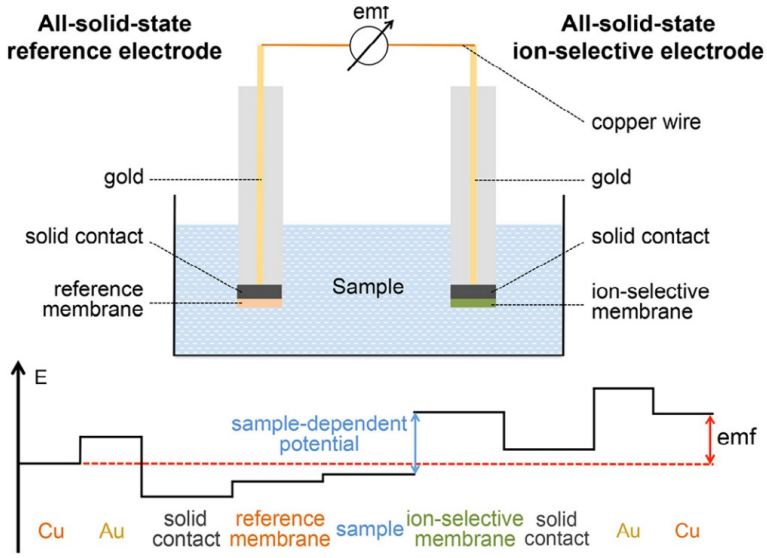

Figure 2.2: All solid state potentiometric cell and the corresponding potential profile of cell showing all interfacial potential differences. Reprinted with permission from [43]. Copyright 2016 Elsevier.

contact and subsequently an ion-selective membrane is deposited. These electrodes are connected to a high impedance voltmeter that measures the potential difference between the two electrodes in near zero current condition. The measured potential as illustrated by the potential profile of the figure is a sum of many interfacial potentials. There are no ohmic potential drops in the system since it operates (ideally) in zero current condition and the only interfacial potential that is dependent on the target analyte activity is the interface between the sample and the ion-selective membrane material.[43]

A conducting polymer acting as a solid contact with ion-to-electron transfer capability is shown in Figure 2.3. Conducting polymers are attractive solid contact materials because they have effective transduction and they can be doped to be both ionically and electrically conductive. The reversible ion-to-electron transduction is achieved through a redox reaction that involves the target and/or its its hydrophobic counter-ion in the membrane. [43, 114] In conducting polymers doped with large immobile anions, the ion exchange mainly involves the exchange of cations at the solid contact membrane interface where small anions doped conducting polymers exchange mostly anions.

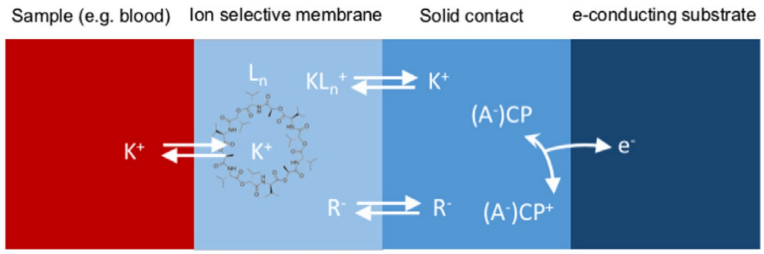

Figure 2.3: Schematic of an ion-to-electron transduction with conducting polymer (CP) doped with anion as a solid contact and with a K^+ selective membrane. L_m is the neutral charge carrier in the membrane with valinomycin ionophore. R^- is a hydrophobic counter ion and A^- is a doping ion. Reprinted with permission from [114]. Copyright 2016 Elsevier.

2.2 Different Electrical ISFET Structures

2.2.1 ISFETs in Unmodified CMOS

A significant step forward in ISFET sensors was the use of unmodified CMOS processes to create pH sensitive arrays.[111, 8, 80] Modern CMOS processes are highly robust, optimized and they allow almost unlimited scalability properties and low power operation making them an ideal component for hand held sensing devices. The unmodified ISFET variant is created by extending the metal gate all the way to the top layer of the chip. On top of this gate a metal passivation layer is deposited. Such an approach allows unmodified CMOS processes to use the passivation layer as the pH sensing layer. This structure is referred as a floating-gate FET (FGFET) and shown in Figure 2.4.

The glass passivation commonly used in the CMOS process is a double layer of SiO_2-Si_3N_4. This layer creates an additional series capacitor and thus a capacitive division at the input reducing the sensitivity.[44] The layer creates poorly defined sensing capacitance as it extends over the entire chip and is usually much thicker than one would design if it could be freely chosen. The use of the passivation layer for sensing also creates threshold variations of several volts between individual sensors due to trapped charge in the passivation layer [77]. Despite the above mentioned drawbacks, the ability to use an unmodified CMOS process improves the reliability considerably and allows mass fabrication, although the encapsulation of the bond wires and electrical part is still necessary before it can be used in a wet environment. The device has been highly successful in applications based on pH measuring such as real-time detection of amplified nucleic acid [111] and in next generation genome sequencing [98]

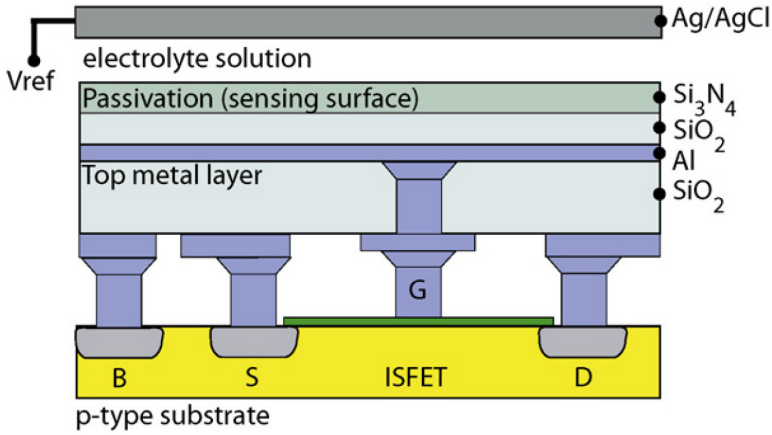

Figure 2.4: pH sensing ISFET fabricated in unmodified CMOS proesses. Reprinted with permission from [31]. Copyright 2009 Elsevier.

2.2.2 Extended-gate ISFET

The most straightforward ISFET structure resembling both conventional ISFETs and the coated wire is the extended-gate ISFET (EG-ISFET) or simply EGFET for general (bio)chemical sensing. Illustration is shown in Figure 2.5. A clear benefit of the structure compared to other ISFETs stems from the separation of the wet and dry environments. This is achieved with extended gate structures where the sensing pad extends off chip and only the sensing pad is immersed into the solution. This makes device fabrication significantly simpler and allows convenient post-processing steps as the surface can be engineered independently from the transducer. The price to pay for the simplicity is clearly smaller. The traces between the electronics and the sensing areas cannot be manufactured as compactly with printed circuit board technologies as with CMOS manufacturing processes. However, for most in situ measurements, the scalability is sufficient. In comparison, coated wire technologies allow high impedance at the sensing interface to translate to a low impedance environment physically significantly closer to the interface than in a conventional coated wire, eliminating commonly used Faraday's cage shielding. In [106], it was realized that the gate oxide does not have to be the sensing membrane. The sensing gate can be extended by applying a conductive medium on top of the gate oxide and the deposition of the sensing membrane on this medium can be used to take the gate far away from the actual transistor.

Recently, this seemingly simple structure has been used for different sensing concepts. A pH sensing demonstration with off the shelf components has been demonstrated [96, 95]. More recently, an electrical ELISA test was shown for detecting BHV-1 specific antibodies produced in cattle in response

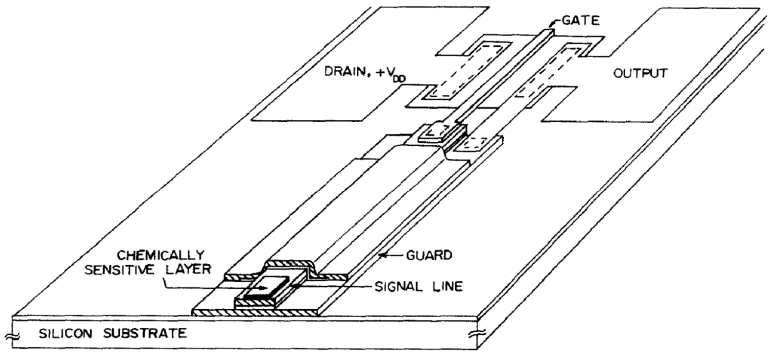

Figure 2.5: Illustration of an extended-gate ISFET. Reprinted with permission from [106]. Copyright 1983 Elsevier.

to viral infection [110]. The extended gate structure has also been used to measure extracellular K^+ concentration with microfabricated sensing pads. In addition, extended gold pads have been used for the detection of DNA [67, 48] and as an enzyme sensor for cholesterol detection [47].

2.2.3 Ion-sensitive Floating-gate FET

The first ISFET using a floating gate (FG) structure with an additional control gate was proposed by Shen et al. [103] and more recently control gate assisted detection has been demonstrated by various groups [74, 5, 6, 57, 58, 122, 56]. Common to these ion-sensitive floating-gate field-effect transistor (ISFGFET) devices is a dual gate structure where one serves as a sensing gate and the other as a control gate as shown in Figure 2.6. Electrically both gates have analogous operation and they are capacitively coupled to a common floating gate. Changes in potential at either one of these gates modulate the floating gate potential. In chemical sensing, one is reserved for control that can be used for biasing and the other gate serves as the sensing gate that is constructed to yield a response from the desired target.

Barbaro et al. [5, 6, 4] presented a charge modulated FET for detection of the intrinsic negative charge of the DNA molecule. The basic principle in Barbaro et al. formulations rely on the assumption that the charged DNA molecules induce a change in the threshold voltage change at the floating gate without the presence of a reference electrode.

Following the work of Shen et al. [103] more recent studies by Jayant et al. [57, 58, 56] have shown that the surface charging can be programed using control gate assisted modulation of the charge at the floating gate. The device was used for pH as well as for DNA sensing. [57, 58] DNA sensing was achieved in three different readout modes including one without a reference electrode. In all modes the achievable surface potential changes are

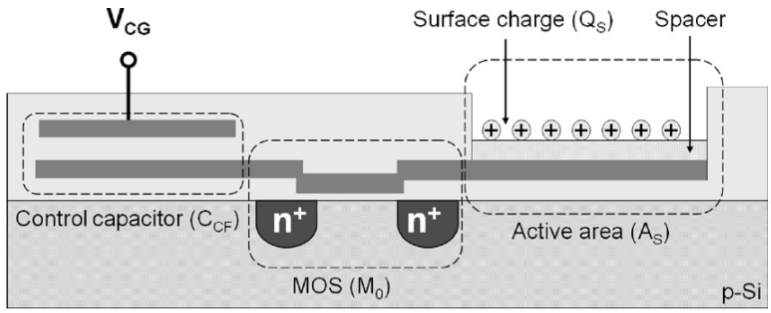

Figure 2.6: Floating gate ISFET with an additional control gate. Reprinted with permission from [5]. Copyright 2006 IEEE.

somewhat larger than usually reported [92, 93]. The reason is not fully understood, but one of the given speculations follows from the ability to change the electric field of the sensing oxide causing a counter ion descreening. Additionally extracellular calcium measurements where recently demonstrated by the same group [56] using the same sensor structure.

2.3 Electrolyte Interfaces

The chemically relevant interfacial potentials in the ISFET are found at the reference electrode-electrolyte and the electrolyte-sensing gate interfaces. The reference should provide a constant and stable potential during operation as it is indistinguishable from any change in the detectable chemical potential. There are a wide variety of different surfaces and their modifications. Oxides are inherently pH sensitive surfaces and are one of the most widely experimentally studied and modeled surfaces. [39, 78, 31] Recent advances with graphene-FETs where the gate material can function as the interfacial sensing material as well as the channel of the FET has increased the interest for graphene functionalizations for detection of proteins and DNA. [118, 81] Gold has been broadly studied because of its ability to form a covalent bond with thiolated DNA probes [42].

Here the potential stability of the interfaces with common pH-ISFET and with ion-selective membranes is briefly discussed. Then the common theory of pH sensing with ISFETs is summarized and followed by the introduction to conducting polymers that provide a promising alternative to (bio)chemical sensing.

2.3.1 Stability of Interfaces

ISFETs are most commonly fabricated using an oxide as the sensing layer. These sensors are known to have a monotonic drift which has been attrib-

uted to buried sites in the oxide layer.[51] These sites are slowly protonated/deprotonated due to hydrogen ions diffusing into the oxide leading to significant monotonc drifts in ISFETs. A correction algorithm can be used after the measurement [40] or more complex hardware based front-end solutions can be employed for directly compensating the non-idealities. [44]

The monotonic drift is commonly strongest when the sensor is exposed to solution after which the potential response starts to stabilize. A separate process from this monotonic drift is the 1/f noise, which also manifests itself as drift via random fluctuations with long time intervals. ISFET manufactured in unmodified CMOS processes have been reported to have significantly more 1/f noise as the corresponding MOSFET in the same die. However, no correlation was found between 1/f noise and the physical dimensions or chemical sensing area of the devices. [77] If charge transport related noise at the insulator-electrolyte interface and reference electrode does not generate noise, then the FET dominates the low frequency noise in the system.[23] However, commonly it is the interface and reference electrode that contributes to the overall noise via charge transport mechanisms. Also significant drifts as well as 1/f noise due to the reference electrode leakage currents has been found [50]. The measured 1/f noise was suppressed after allowing the sensor to stabilize for several hours indicating reduced monotonic drift. The currents are expected to influence the device operation because of finding parasitic paths to the device or measurement set-up.

One widely neglected issue in most FET based sensing applications is the requirement of a stable reference electrode. To date, reference electrodes are still bulky and often fragile. The stability requirement is relaxed in applications where only a change of potential is measured against some predetermined threshold yielding a semi-quantitative yes/no answer about the presence of a specific target in the sample. Recently, notable performances have been achieved with Ag/AgCl elements covered with a mixture of a KCl salt and a polymer. [113] The reference electrode remains within ± 0.5 mV in 0.1 M KCl over two months and has high stability against electrolyte concentration changes.

In electrochemical sensors it is important to understand a fundamental property where the measured chemical target is not for the most part directly electrical but, for example, ionic. All such electrodes including the reference electrode are asymmetric in a sense that the ions do not enter the electronic readout device. Therefore, at some point in the system there needs to be transduction from an ionic signal to an electronic signal via a reversible redox reaction. A common redox reaction used in an Ag/AgCl electrode in contact with chloride ions reads [15]

$$Ag + Cl^- \rightleftharpoons AgCl + e^- \tag{2.5}$$

The transduction mechanism of ion-to-electron is analogous to the above reaction even with different materials such as polyaniline. The electrodes have a finite amount of redox sensitive material, which leads to finite redox capacitance C and can be presented as

$$\frac{\Delta V}{\Delta t} = \frac{i}{C} \tag{2.6}$$

where i is a constant current and V is the electrode potential changing in time t. C is complemented with a small series R that will shift the potential by a constant amount

$$\Delta V = iR \tag{2.7}$$

This simple RC model reveals the main idea behind the ion-to-electron transduction. In high impedance potentiometers, current induced potential differences can be neglected, but currents induced by electrical noise may lead to changes in the measured potential. When these electrodes are miniaturized it tends to increase R and decrease C. This leads to lower potential stability.[15] Regardless, solid contact microelectrodes have been successfully employed, for example, to measure the Martian soil for various ion concentrations [72] as well for potassium concentration measurement in a rodent brain [90]. Miniaturization obviously makes the construction of arrays more sensible and such configurations have shown to overcome some selectivity limits of a single sensor [84].

As a side note, it is a common practice in biosensing to replace the bulky reference electrode with inert metals such as Pt or Au. These materials do not have well-defined electrode reactions and therefore using these electrodes for gating the device can result in significant potential instabilities. [21]

2.3.2 pH Sensitivity of Oxide Interfaces

The pH response was originally described using the Nernst equation, and experiments commonly exhibit sub-Nernstian slopes. More advanced theories consider a double layer that describes the electrolyte solution as the capacitance and the surface charge is explained through the site binding model, which assumes the amphotheric binding sites at the surface. It was realized that the simple capacitor equation, V=Q/C, yields results close to those experimentally observed [39, 38]. Subsequent efforts are usually either modifications or extensions to the well established theory summarized below [57]

$$\frac{\partial \Psi_0}{\partial pH_B} = -2.3\frac{kT}{e}\alpha \tag{2.8}$$

$$\alpha = \left(\frac{2.3kTC_{DL}}{q^2\beta_{int}} + 1 \right)^{-1} \tag{2.9}$$

$$\beta_{int} = 2.3H_S^+ N_S \frac{K_B H_S^{+^2} + 4K_A K_B H_S^+ + K_A K_B^2}{(K_A K_B + K_B H_S^+ + H_S^{+^2})^2} \tag{2.10}$$

$$C_{DL} = \frac{C_{diff} C_{Stern}}{C_{diff} + C_{Stern}} \tag{2.11}$$

The sensitivity coefficient α can have values from 0 to 1. From 2.9 we observe that a Nernstian ($\alpha \approx 1$) requires a high buffering capacity β_{int}. The buffer capacity is strongly dependent on the density of the ionizable groups N_S, which has a key role in determining the slope of the response. Additionally, although not directly clear from Eq. 2.10, the buffer capacity has the largest changes near the point of zero charge described with a characteristic pH value $pH_{PZC} = (pK_A + pK_B)/2$. The high buffer capacity is achieved with a high ionizable group density or by having a small separation between the surface dissociation constants $\Delta pK = pK_B - pK_A$. It is concluded by [38] that with high buffering capacity the C_{DL} has only a modest impact on the overall response. For sub-Nernstian surfaces, the impact can be more significant and this parameter can be only controlled via the ionic strength of the electrolyte. For pH sensitive ISFETs, the high buffering capacity minimizes the effect of the ionic strength of the electrolyte. While a smaller ΔpK achieves increased density of ionizable groups at the surface around the PZC improving the pH response. The decreased N_S on the other hand reduces the α and thus the pH sensitivity via the reduction of sites that can achieve proton binding [57]. The PZC remains independent from the varying N_S.

2.3.3 Conducting Polymers

One of the intriguing emerging materials are conducting polymers with a large diversity of possible applications. The importance of these materials have been recognized by the scientific community when Hideki Shirakawa, Alan J. Heeger and Alan G. MacDiarmid were awarded the Nodel prize in chemistry in 2000. The first conducting polymer, aniline black (polyaniline), was obtained over 150 years ago as an oxidation product of aniline. However, the electrical properties where not established at that time and a discovery of conducting polymers is attributed to doping of polyacetylene in 1976, which showed a unique combination of properties different from all other known materials. [14].

Polyaniline (PANI) and its derivatives is among the most extensively studied polymers. [24] The research has progressed from basic studies con-

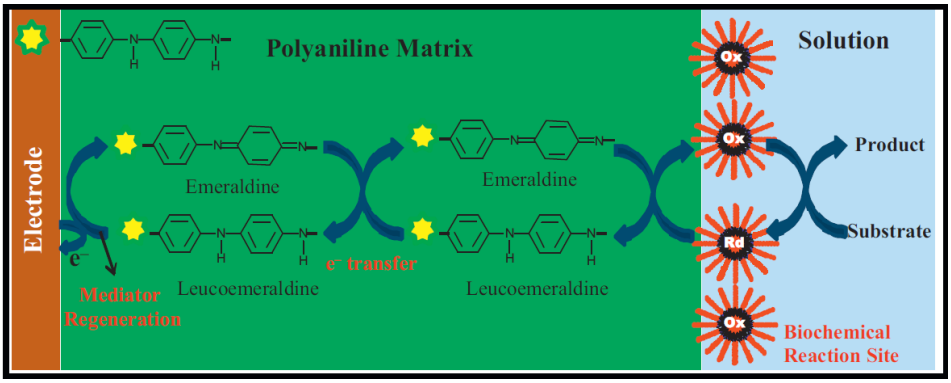

Figure 2.7: Electron transfer process from a biochemical reaction with polyaniline acting as a mediator layer between the reaction and the electrode surface. Reprinted with permission from [24]. Copyright 2011 Elsevier.

cerning properties such as conductivity, stability, and processability to applications including (bio)chemical sensing.[123] The multifunctionality of the material is partly a result of the polymers backbone that can include many possible substituents and possible doping ions or neutral molecules trapped inside the polymer matrix. The electroactivity of the materials means that the properties are dependent on the oxidation (p-doping) or reduction (n-doping) of the conjugated polymer backbone. Polyaniline is promising in (bio)chemical sensing due to its ability to function as an immobilization matrix and due to its ability to translate a chemical signal into an electric signal. Moreover, a molecular recognition layer can be to attached to the polymer.[14]

PANI exhibits two redox couples in the potential range for enzyme-polymer charge transfer and therefore acts as a self-contained electron transfer mediator, i.e., no additional mediators such as ferricyanide, ferrocene derivatives, organic dyes, etc. are needed. [24] The electron transfer process is shown in Figure 2.7 where PANI acts as the mediator layer between the biochemical reaction and the electrode surface. Additionally, PANI is compatible with biological molecules in neutral aqueous solutions and therefore promising in biosensors relying on matrix entrapment of biomolecules. [87]

Many conducting polymers including PANI show ionic response, redox response, and pH sensitivity. However, their applicability to biosensors interacting with biological macromolecules can be challenging. Therefore, PANI should be functionalized in a way that enhances the selectivity toward the intended target while minimizing the selectivity toward any other chemical/biological parameter such as pH.

The conjugated polymers can be used as an ion-to-electron transducer. A key parameter affecting their performance in this respect is the redox

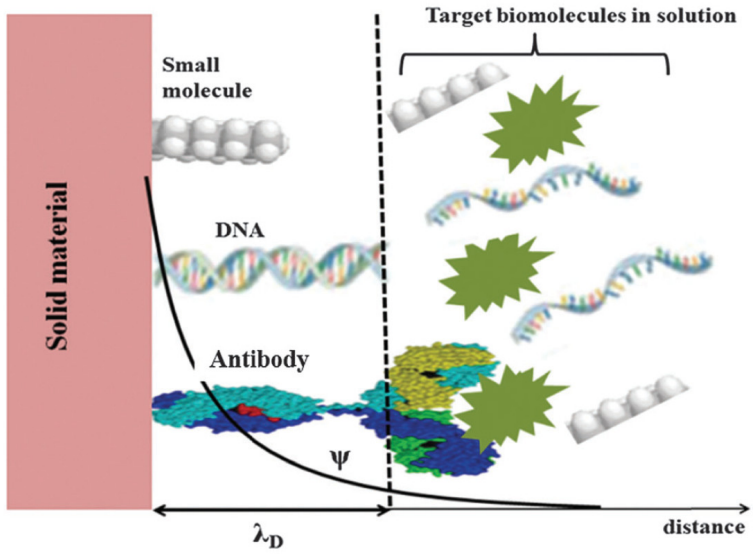

Figure 2.8: Electrical double layer length shown in the presence of different targets. The dimensions are not scale. Reprinted with permission from [45]. Copyright 2015 Royal Society of Chemistry.

capacitance. PANI for example is a conjugated polymer that is quite stable in its highly oxidized (p-doped) state and has high electronic conductivity and high redox capacitance. The high redox capacitance makes it efficient in ion-to-electron transduction. However, there might be electro-chemical side reactions where for example O_2, CO_2 and H_2O_2 can reach the polyaniline (solid contact) even when it is coated with an ion-selective membrane. [15]

2.3.4 Double Layer Screening

Among the widely debated issues is the detection of biomolecules in a label free fashion. Originally it was believed that since many biomolecules carry intrinsic charge these molecules could be detected with field-effect devices. Despite significant efforts, the results did not prove satisfactory due to the electrical double layer. [99] In ionic solutions, small ions carrying a charge opposite to the detectable large macromolecule create a cloud of opposite charge around the macromolecules effectively screening the net observed charge. The impact of screening is dependent on the distance between the surface and point of observation. The amount of observed charge is characterized by the Debye screening length

$$\lambda_D = \sqrt{\frac{\epsilon_w \epsilon_0 kT}{2z^2 e^2 n_0}} \tag{2.12}$$

where ϵ_w is a dielectric constant of the solution, ϵ_0 is the vacuum permittivity, k is the Boltzman constant, T is the temperature, z is the valence of ions, e is the elementary charge. n_0 is the bulk ion number density related to the ion concentration c_0 in units of M as $n_0 = 1000 \times N_A \times c_0$ where N_A is the Avogadro constant. [49] At distance of one Debye length the electrical signal has decayed to 1/e of its original value.

Typical screening lengths are in the order of 1 nm unless very diluted solutions are considered. This is considered to be the main reason limiting label free biosensor development.[45] Figure 2.8 depicts the electrical double layer length compared to the size of several biomolecules. The larger the molecule the stronger the screening effect (figure not to scale). Additionally, linking the capture molecule to the surface commonly requires some linker molecules that increases the target molecule distance even further.

Recent efforts for overcoming the screening effects include both electric field based enhancement as well as direct interfacial modifications. A straightforward modification was achieved by Jang et .al [55] where a FET based sensor was combined with alkaline phosphatase labels that induced Ag precipitation yielding Debye screening free detection. Such a system is more complex from the user point of view since it uses labels, but has a potential for faster commercialization as it relies on more established technologies. Moreover, the limit of detection is claimed to be lower than conventional ELISA. More scientifically novel concepts circumventing the screening were done in a label free manner by Kulkarni et al. [73] by operating the sensor at high frequencies. A high frequency applied to the sensor source terminal is expected to breakdown the electric double layer (EDL) charge screening and allow the detection of fluctuating biomolecular dipoles rather than the charges directly. The drawback of the proposed mechanism is more delicate and complex electronics to drive the sensor. Also the system is demonstrated via carbon nanotube FET and the generality beyond nano devices is unclear. A somewhat similar idea was demonstrated by Goykham et al. where biomolecular interactions where detected using receptor dipole properties. [35]. Gao et al. [30] modified the nanowire FET gate interface with a porous biomolecule permeable polymer layer. The layer increased the effective Debye screening length and thus enhanced label free detection [30].

2.4 Detection Mechanisms with FETs

2.4.1 Ion Detection with ChemFETs

When ISFETs are modified to be chemically sensitive to ions other than H+, these sensors are called ChemFETs [100]. The key component that determines the selectivity of the ion over other interfering ions is the ion selective membrane (ISM). An ion selective membrane creates a non-polarized

interface with the solution. Ideally the interface is permeable to specific ion only and the potential difference at the interface is expressed via the Nernst equation

$$V_{cell} = V_{cell}^{0} + \frac{RT}{z_i F} \ln a_i^S \tag{2.13}$$

where the interfacial potential V_{cell} consisists of constant standard potential V_{cell}^{0} and the ion activity a_i of species i in the sample phase S and z_i describes the number of charges per ion. The constants R, T and F are the universal gas constant, temperature, and Faraday constant respectively. The resemblance to ISFET formulations is clear as they are in principle the same.

ISFET development for other ions has followed the development of macroscopic ion selective electrodes (ISE).[54] The macroscopic sensors that operate in an analogous principle to ISFETs are the oldest class of chemical sensors.[54] ISEs have been applied in many fields including biomedical and environmental monitoring. In many cases they provide excellent performance compared to other types of sensors. The measurement of biologically relevant electrolytes in body fluids is still a key development area for ISE research and billions of measurements are done globally each year. Additionally, potentiometric sensors measure the ion activity rather than the concentration. This is beneficial in health related applications where health disorders are commonly related with activity.[125]

In addition to miniaturization, the current trends in research are aimed at developing new ionophores with higher selectivity and lipophilicity with ISEs working in direct contact with blood samples. [2, 113] Miniaturization of analyzers and solid-state reference electrodes are required for fully integrated sensor constructions. Although ISFETs are promising technology for the transducer, they are not yet commercially available for clinical chemistry applications. The common problems are the encapsulation of the FET, and insufficient adhesion of polymer membranes to the gate.[2]

Recent publications in ChemFET include a miniaturized multi-sensor chip for direct detection of pH, potassium, sodium, and chloride ions in blood serum.[2] The selectivity was achieved using ion selective membranes. The same technique was applied to natural mineral water analysis and the applicability for sensing in real samples was shown.[46] Ion channel screening of cells with an ISFET array was demonstrated recently [116] and a CMOS chip for detection of E.coli bacteria via potassium sensitive FETs was explored. [89]

2.4.2 Direct Detection of Macromolecules

The oligonucleotide is a much smaller macromolecule than a protein. Thus, the Debye screening effect does not affect the detection of DNA as strongly.

This has attracted a significant amount of interest in the scientific community because of the potential of label free detection in molecular diagnostics.[93] An oligonucleotide probe based DNAFET, shown in Figure 2.9, can be constructed by immobilizing specific probes on the transistor gate. The complementary strand of the probe will hybridize with a high specificity to the complementary strand and thus highly selective sensors can, atleast in theory, be constructed. The negatively charged DNA backbone creates a threshold voltage shift upon detection. The length of the DNA molecules base is about 0.34 nm and thus at least a part of a DNA probe's charge is seen at the gate surface with practical salt concentrations that allow sufficient hybridization efficiency. [103]

The sample can contain several important targets to be detected. Transistor based sensors are especially well suited for multiplexed detection of several targets in one reaction as they can be constructed to be fully independent in operation. This is achieved simply by incorporating several transistors in one array with different DNA probes. Label free probe based DNA hybridization detection via miniaturized transistor systems has been shown on several occasions [112] [29] [48] and also DNA microarrays with direct hybridization detection.[85, 4, 12]

FET based sensors using uncharged PNA probes have also been recently investigated [34]. The PNA probes are expected to yield enhanced detection as electrostatic repulsion between probe and target are eliminated and hybridization can be achieved in lower salt concentrations. Control gate assisted detection was demonstrated with an ability to create eletrostatistical aid or repulsion of DNA immobilization. [58]

A critical review of direct DNA detection, however, concluded that although label free detection should be possible, there is a wide variability of empirical results about the changes in the gate potential resulting from DNA hybridization.[92] Additionally, the theoretical understanding was not considered to be adequate and the predictions do not match well with the experiments. Although the report was written more than a decade ago, the fundamental understanding behind the observed measurement results still remain unclear. [93]

Similarly, the direct label free detection of antibody-antigen interactions has attracted a lot of interest. Proteins are charged molecules with the exception that in a certain characteristic pH levels they carry zero net charge. Due to the intrinsic charge it was originally thought that these molecules could be detected via surface charge sensing devices. Whether or not this is possible has been debated. The reason for unsuccessful detection has been considered to be double layer screening.[21, 99] However, several reports claim successful label free detection, for example antibody-antigen complexes where the size of the complex is at vastly longer distances than the electric double layer described in a recent review. [93]

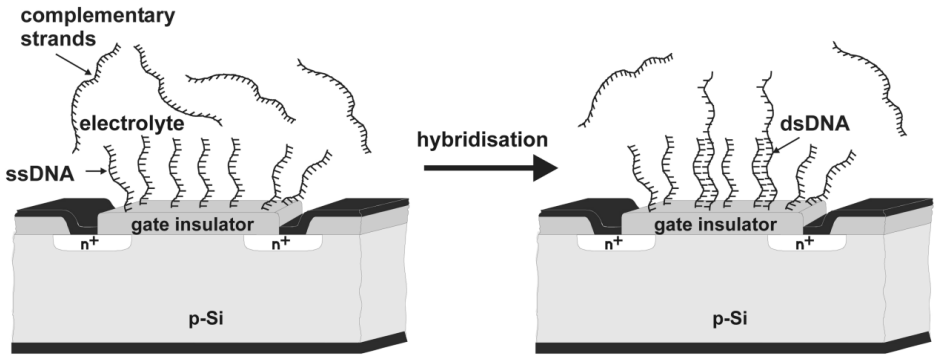

Figure 2.9: Label free detection of DNA based on the intrinsic negative charge in the DNA backbone. Reprinted with permission from [100]. Copyright 2002 Royal Society of Chemistry.

One commonly used explanation for the observed results is the Donnan effect.[21] According to this theory, proteins are considered as a membrane on the electrode surface. Small ions can shuffle between the solution and this protein layer membrane. When a fixed charge is present due to the target, a difference in ion concentration develops between the membrane and the solution. This redistribution of ions creates a detectable change in the interfacial potential of the membrane and the solution. A change in this Donnan potential also causes a shift in pH. The total response is the combination of the surfaces pH response and the Donnan potential. According to this theory, a Nernstian surface fully compensates the protein binding induced changes and a non-Nernstian surface is required for successful detection. [99, 21]

2.4.3 Indirect Detection of Macromolecules

Directly measuring the intrinsic charge using FETs is difficult and the performance is limited due to several issues. The double layer screening limits the net observable molecular charge. The shape of the DNA molecule also plays a part as the change in the charge distribution. It is generally considered that a single stranded DNA takes a Gaussian shape whereas a double stranded DNA has a rod like shape. Therefore, it is unclear if a change in charge or shape is detected or if it is a mix of different phenomena.[86]

An alternative approach to enhance the signal and by a large part remove the screening problems is to use redox sensitive surfaces and labels. Usually enzyme labels can be used that react with the sensing surface. For example, in DNA detection ferrocenyl-alkanethiol modified gold electrodes exhibit larger dynamic range and significantly improved long term drift compared to the direct detection mechanism.[86] A common practice for antigen detec-

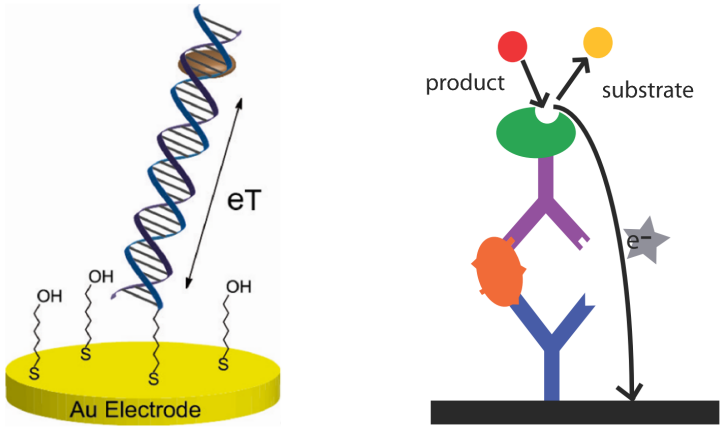

(a) (b)

Figure 2.10: a) Label assisted detection of DNA with redox label. Electron transfer reaction takes place between the surface and the DNA that is tethered to the gold surface via alkanethiol linker. [1] b) Electrical sandwich ELISA type of configuration where the labelled secondary antibody interacts with surface via electron transfer. Reprinted with permission from [36]. Copyright 2008 MDPI.

tion is to conjugate an enzyme label to a secondary antibody that specifically binds to the detected antigen [124]. Figure 2.10 illustrates the detection of a DNA a), and antigen b), with the help of labels that react with the surface via an electron transfer process. However, such modification, even if beneficial for more robust sensing, generally requires labels and more complicated sample preparations and measurement devices.

Enzymes can also function directly as a recognition layer. Enzyme-FETs (EnFETs) are usually created by immobilizing an enzyme to the FET gate. For the immobilization, a number of techniques are available such as physical and chemical absorption, entrapment within polymeric matrices, covalent binding, cross-linking and mixed physiochemical methods.[100] The first enzyme based ISFET was created by having a membrane deposited on the gate with cross-linked penicillinase. When penicillin is present in the sample the enzyme catalyses the hydrolysis of penicillin to penicilloic acid. Protons released during the reaction change the pH near the gate that can be detected. [101, 25]

An alternative for pH based sensing enzyme detection can be achieved with, for example, organic polymers that accommodate effective electron transfer properties allowing direct detection of enzymatic or redox reactions.[97] The enzyme polymer charge transfer for polyaniline is depicted in Figure 2.7. Additional mediators are not required for electron transfer. This

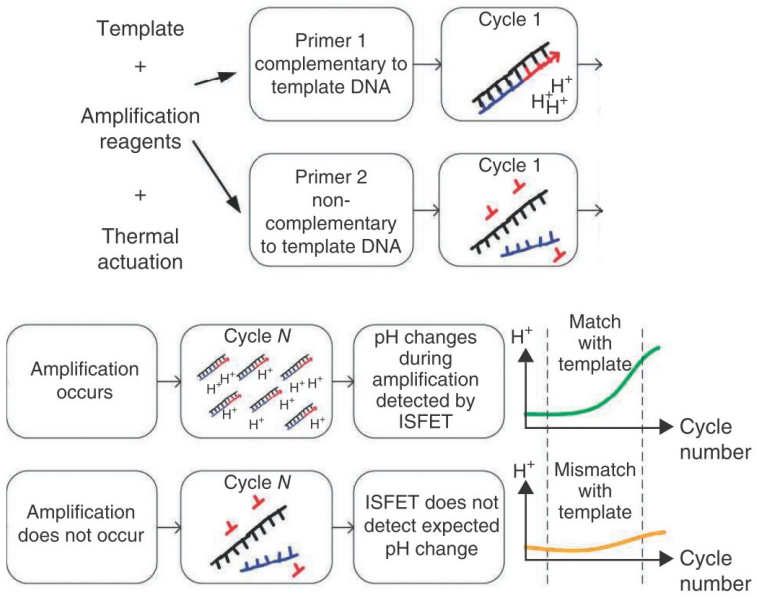

Figure 2.11: Label detection scheme using ΔpH as the indicator of growing DNA strands when nucleotides are incorporated into the template DNA releasing hydrogen ions. Reprinted with permission from [111]. Copyright 2013 Nature Publishing Group.

can be used for creating a fairly simple sensing system towards stand-alone devices. [24]

Another pH mediated detection scheme recently described [111] employs a polymerase chain reaction (PCR) on chip and detects released hydrogen ions when nucleotides are incorporated to the growing DNA strands [111]. The local temporal shift in the H^+ concentration in the ISFET results in a change in the ISFET surface potential. A sufficient number of DNA templates are achieved using PCR amplification where the amount of DNA strands grow exponentially. The specificity of the system is created by the primer that is required to initiate the PCR and which can be designed to bind only to a specific target. After a sufficient amount of amplification, the hydrogen ions released can be detected while the amplified templates are grown into double strand structures. This detection scheme using pH as the indicator is also found in the Ion Torrent next generation sequencer [98].

Chapter 3

Aims of the Study

The original publications had the following aims:

I Surface functionalization of ion sensitive floating gate field effect transistor with organic electronics
In this study the aim was to explore a new sensing concept of the developed CMOS based ISFGFET sensor structure as well as the applicability of organic polymers as a functionalization layer deposited directly on the sensor. A successful organic polymer functionalization could allow the many attractive (bio)chemical sensing properties to be transferred to the ISFGFET sensor.

II An Ion-Sensitive Floating Gate Field-Effect Transistor Model: Operating Principles and Electrofluidic Gating
Understanding the structure and properties of the electrolyte solution and the sensing surface interface is the key for advancing new sensor applications and sensing mechanisms. This study aims to develop a robust and self-contained model that describes the ISFGFET operating principle and its possibilities beyond the conventional ISFET. The work introduces a new concept for field-effect sensing: electrofluidic gating that allows for electric field manipulation of the charged solution.

III Compact Model and Design Considerations of an Ion-Sensitive Floating Gate FET
This is a continuation study of (**II**) where the aim is to further elaborate the design trade-offs between ISFGFET properties. This is achieved by creating an intuitive model and integrating it into a computationally efficient simulation tool. This allows the evaluation of the sensor in a larger array and the parasitic effects can be included efficiently as a part of standard electronic circuit simulator tools.

IV Low-Cost Chemical Sensing Platform with Organic Polymer Functionalization

Chemical sensors are usually based on some custom manufacturing processes and additionally require substantial manual work. This study aims to circumvent that problem by using standard electronic manufacturing processes and electronic components when creating a low-cost disposable sensor solution. In this study the applicability of extended gate ISFETs with PANI functionalization are explored and compared to conventional electrodes.

V Hand-held transistor based electrical and multiplexed chemical sensing system

For applications that need to generate information in-situ and transmit it from a distance, it is imperative to have a system that can measure many different targets simultaneously. The sensing needs to be achieved with a portable device with cloud connection and by using a disposable sensing element for the detection. This study is a continuation of (**IV**) and aims to create a general ISFET based sensing system for a wide variety of potentiometric sensing applications. The hand held battery powered device for remote monitoring is designed using a mobile phone initiated measurement which allows cloud based information sharing. Importantly, the system utilizes a low-cost disposable sensing platform.

Chapter 4

Materials and Methods

The most relevant aspects of material and methods are presented in this chapter. More details can be found from the original publications.

4.1 ISFGFET Device Fabrication

The chip was manufactured through MOSIS in California with the 0.25 μm double polysilicon gate CMOS process (**I, II** and **III**). The chip was encapsulated with PDMS to protect the bonding wires. The overall dimensions of the chip are 5 mm x 5 mm. The individual sensors have glass passivated during the manufacturing process. The passivation consists of a 0.5 μ thick SiO_2 layer followed with a 1 μm Si_3N_4 layer deposited on top. The passivation layer was etched using reactive-ion etching (RIE) that exposed the underlying aluminum sensing pads. A thin layer of native Al_2O_3 oxide formed on the surface with an expected thickness of 6 nm. This surface was used for pH sensing studies. For polyethyleneimine (PEI) sensing studies, the device was functionalized with conductive, polyaniline/dinonylnaphthalene sulfonic acid (PANI-DNNSA). The functionalization was achieved by coating it with PANI-DNNSA by drop casting a 0.5 μL wt% PANI-DNNSA on top of the chip and drying for a minimum of 2 h under vacuum.

4.2 EG-ISFET Construction

An ISFET sensing platform was designed by combining a discrete n-type MOSFET and a custom printed-circuit-board (PCB) (**IV** and **V**). The platform material was FR4 with gold traces. The gold plating was achieved by electroless nickel immersion gold (ENIG) surface plating and the traces were encapsulated with liquid photoimageable solder mask. The sensing pads were extended from the transistor gate, and the sensing pads can be immersed in

solution while leaving the transistors in air. This eliminates any transistor encapsulation problems. The transistors were soldered into the platform.

4.3 Chemicals and Electrode Preparations

PANI-H_3PO_4 (IV) : Aniline (Sigma Aldrich) was purified by distillation under reduced pressure. Ammonium peroxidisulfate (Sigma Aldrich) was used without additional purification. 10 mL of 0.1 M solution of aniline in 1 M HCl was mixed together with 10 mL of 0.125 M solution of ammonium peroxidisulafate in 1 M HCl. The reaction mixture was briefly stirred and left overnight to complete the polymerization. Then the black-green precipitate was separated by filtration, washed with water and acetone until the washing liquids became colourless and deprotonated overnight with 10 wt.% ammonia water. The deprotonated PANI (in emeraldine base form) was again washed with acetone and dried in the air. The dried sample then was dissolved in N-methylpyrrolidone to produce 7 wt.% solution.

The used buffer solutions were pH 7 phosphate buffer and pH 4 citrate buffer purchased from FF-Chemicals. The pH 1 (1M HCl) was prepared by dilution of concentrated hydrochloric acid. All the aqueous solutions were prepared with the use of deionized water (18.2 MΩ cm^{-1}, ELGA PureLab Ultra system). The same preparation process has been described earlier [17].

The prepared solution of PANI in N-methylpyrrolidone was drop-casted onto the gold surface of the platform sensing pad and dried in air for 2 days. The dried film was placed into 1M solution of orthophosphoric acid in order to convert the emeraldine base form of PANI into emeraldine salt, having dihydrophospates as counterions to the charged nitrogen atoms, PANI-H_2PO_4.
PANI-DNNSA (I,V): Polyaniline-dinonylnaphthalenesulfonic acid (PANI-DNNSA) was purchased from Crosslink Inc. and used without additional purification. PANI-DNNSA was dissolved in chloroform to obtain 1.5 wt.% dispersion suitable for drop casting. Chloroform (purity >99 %) containing ethanol as a stabilizer was obtained from Sigma Alrdich. in (V)The polyaniline was deposited by drop casting 8 μL of PANI-DNNSA 1.5 wt.% dispersion in chloroform onto each sensing pad and left drying overnight. Several membrane configuration were tested as explained in detail in (**V**). Briefly, the simplest case did not utilize the polyaniline layer and only the ion-selective membrane was casted on gold. The second configuration used the PANI-DNNSA as described above. In the third studied variant, the platforms were placed in 70% ethanol for 1 min to remove the excess DNNSA and improve the electroactivity of the material [70]. In (**I**) 0.5 μL of 1 wt PANI-DNNSA was drop casted on the chip surface and left drying under vacuum for a minimum of 2 hours.
Ion-selective membrane (V): Selectrophore ® grade potassium ionophore

I (Valinomycin), potassium tetrakis [3,5-bis(trifluoromethyl) phenyl] borate (KTFPB), dioctyl sebacate (DOS) and high molecular weight polyvinylchloride (PVC) were purchased from Sigma Aldrich. Tetrahydrofuran (THF) was obtained from Fluka. Sodium chloride (ReagentPlus, Sigma Aldrich) and potassium chloride (Riedel-de-Haen) were used to prepare solutions of primary and interfering ions, respectively.

Lyophilized serum, Nortrol ®, Thermo, containing 3.8 mM of K^+ and 147 mM of Na^+, were recovered from lyophylizate by adding the required amount of deionized water. Deionized water (18.2 MΩ cm, ELGA PureLab Ultra system) was used for preparation of all aqueous solutions.

The K^+-selective membrane was prepared by dissolving 1.57 mg of potassium ionophore I, 0.78 mg of KTFPB, 102.29 mg of DOS and 52.24 mg of PVC in 1 mL of THF. The obtained solution was shaken briefly using the vortex mixer and left on a nutation platform overnight to ensure dissolution of PVC. The platforms were cast with 17.2 μL of the K^+-selective membrane solution and dried overnight.

Chapter 5

Summary of Results and Discussion

5.1 (Bio)chemical sensing with ISFGFET

A simplified cross-sectional view of the ISFGFET functionalized with polyaniline is shown in Figure 5.1. The sensors have a dual gate structure and both of them are capacitatively coupled to a common floating gate (FG). The floating gate (FG) can be considered as the gate of a typical n-type MOSFET. The FG potential (V_{FG}) can be modulated by either the control gate (CG) or by the sensing gate (SG). The sensing gate is immersed into the electrolyte solution. Any change in the electrochemical cell potential arising from the reference electrode or in the membrane potential during sensing, for example, modulates the FET channel conductance by coupling through the FG. Similarly, a multipurpose CG can be used to modulate the channel conductance and also set the operating point of the transistor. If, for example, an ion-sensitive membrane is applied to the sensing gate and the charging at the surface changes in response to some specific chemical target, the change in potential at the FG can be detected via modulation of the threshold voltage.[74] The functionality of the CG will be explored in detail within this chapter.

The device operation principle is explained in more detail using the models in Chapter 5 where the possibilities to modulate the FG potential are considered. Origins of the Ψ_0 are explained. The device design is described in (**I**) [122].

5.1.1 Working Principle of the Functionalized Device

Conducting polymers are advantageous materials for construction of biosensors because of their high bandgap sensitivity, possibility for nanoscale surface area and versatile surface bioconjugation strategies. In (**I**) the aim was

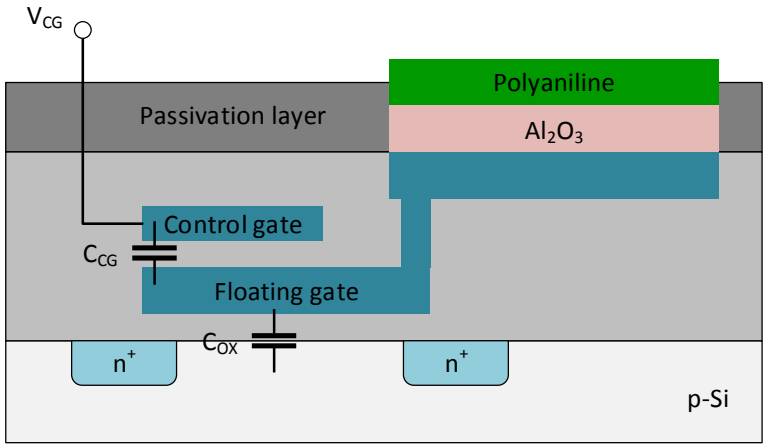

Figure 5.1: Simplified illustration of the ISFGFET. Adapted from (**I**)

to investigate if polyaniline could be used to functionalize the ISFGFET. Additionally, the device structure employs an additional control gate that can be used to bias the transistor. It has been presented earlier that operation without the reference electrode is possible [5] [6] [58]. This is important as the presence of the reference electrode remains a major inconvenience and to date reliable miniature reference electrodes do not exist. The possibility to operate the device without the reference electrode was also examined.

The following charge induction model can be used to qualitatively asses the ISFGFET behavior without the reference electrode. The charge at the FG can be expressed as

$$C_{CG}(V_{FG} - V_{CG}) + C_{OX}V_{FG} + Q_i = Q_0 \tag{5.1}$$

where C_{CG} is the CG capacitance, C_{OX} is the channel gate oxide capacitance, V_{CG} is the CG potential, V_{FG} is the FG potential, Q_0 is the initial trapped charge in the FG and Q_i is the induced charge effect from the SG. The floating gate potential can be expressed as

$$V_{FG} = \frac{C_{CG}}{C_{TOT}}V_{CG} + \frac{Q_0 - Q_i}{C_{TOT}} \tag{5.2}$$

where $C_{TOT} = C_{CG} + C_{OX}$. Parasitic capacitances in the device are omitted for simplicity. With the perfect induction hypothesis followed here $Q_i = -Q_S$ [5]. The change in threshold voltage can be obtained from the relationship

$$\frac{C_{CG}}{C_{TOT}}V_{CG} - \frac{C_{CG}}{C_{TOT}}V_{CG}^T = V_{FG} - V_{FG}^T \tag{5.3}$$

where V_{CG}^T is the threshold voltage seen from the CG and V_{FG}^T is the threshold voltage at the FG, i.e., the single gate transistor threshold voltage. This is CMOS process dependent and usually obtainable from the foundry specific SPICE parameter list. Introducing Eq. 5.2 into Eq. 5.3 with the charge induction hypothesis yields

$$V_{CG}^T = \frac{C_{TOT}}{C_{CG}} V_{FG}^T - \frac{Q_0 - Q_i}{C_{CG}} = \frac{C_{TOT}}{C_{CG}} V_{FG}^T - \frac{Q_0 + Q_S}{C_{CG}} \tag{5.4}$$

Finally, the change in the threshold voltage due to the induced surface charge can be obtained by differentiating the above

$$\Delta V_{CG}^T = \frac{\Delta Q_i}{C_{CG}} = -\frac{\Delta Q_S}{C_{CG}} \tag{5.5}$$

Therefore, an increase of the positive (negative) net charge on the sensing surface will result in a decrease (increase) in V_{CG}^T. Then, changes in V_{CG}^T induced by a recognition event in the sensing surface can be used as the indicator of the reaction. The threshold voltage can be measured by sweeping the gate voltage at a fixed drain voltage continuously measuring the drain current and then extracting the intercept point.

The chip described in (**I,II** and **III**) was manufactured by the 0.25 μm double polysilicon gate CMOS process and the encapsulations were achieved with PDMS. During the manufacturing a glass passivation layer is deposited on top of the chip. This layer was etched away using reactive-ion etching (RIE) that exposed the underlying aluminum sensing pads. To this pad, a native Al_2O_3 oxide forms with a thickness of $\approx$ 6 nm.

5.1.2 Experimental Results of the Functionalized Device

The functioning of the polyaniline modified device was tested using a polyethyleneimine (PEI) which is a polycationic electrolyte that can deprotonate PANI. The primary and secondary amines of PEI can absorb protons from PANI-DNNSA changing the charging at the surface. Increasing concentrations of PEI was dropped on the surface coating causing deprotonation. The surface was dried in air for 2 h and the threshold voltages were measured. The results are given in Figure 5.2. The increasing V_{CG}^T indicates decreased interfacial potential as expected since the PEI deprotonates the PANI-DNNSA. A comparison study was performed using a conventional OCP under aqueous conditions. The measurement confirms that the PEI creates more negative charge at the sensing PANI-DNNSA interface. The measurement conditions are clearly different where the ISFGFET was operated without the reference electrode and in solid state whereas the OCP was measured in a solution with a reference electrode. The reaction and surface conditions are the same yielding qualitatively comparable results.

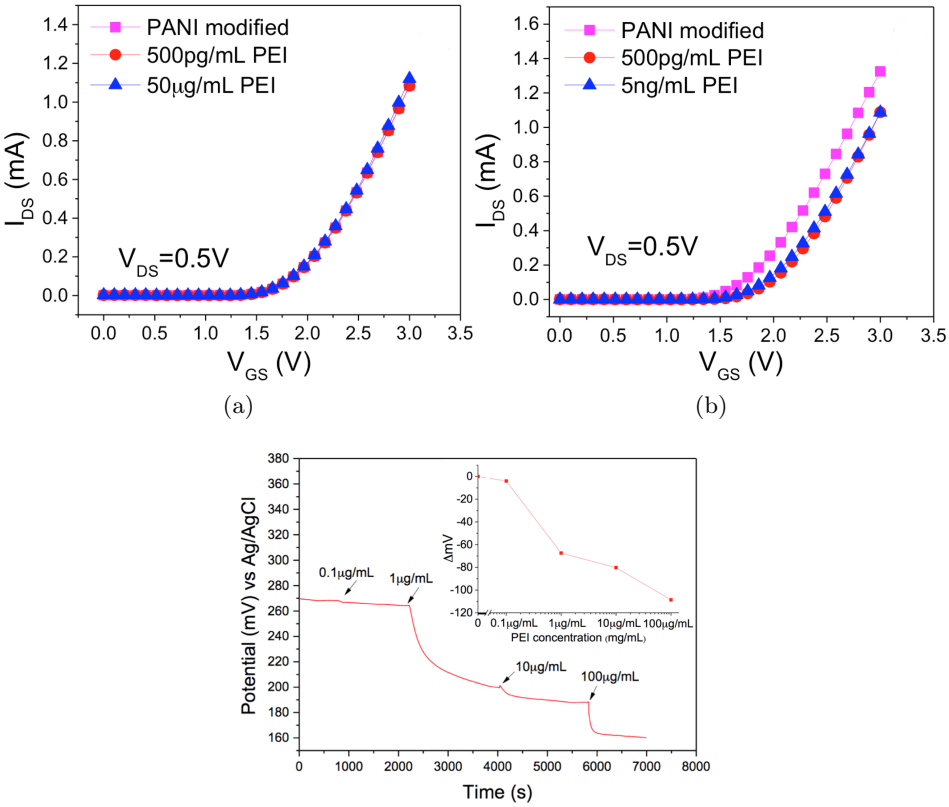

Figure 5.2: Transfer characteristics of PANI-DNNSA functionalized device in PEI sensing with the passivation layer uncut a) and with passivations layer cut b). In c) the same reaction tested under OCP with GC electrode. (**I**)

5.1.3 Electrofluidic Gating

The behavior of pH sensitive ISFETs has been widely studied both experimentally as well as theoretically. The earlier models approximate the sensors by uncoupling the sensing surface from the underlying field-effect device. [18, 39, 38, 78] Recently, however, it has been found that the ability to control the electrolyte solution via the field effect can lead to new intriguing possibilities in fluidic devices such as electroosmotic flow, control the transport of charged proteins, and charge regulation of nanopores. [61, 60, 32, 108, 68]. This ability is not available in conventional ISFETs nor can it be predicted with models presented earlier. Here the focus is on finding a fundamental understanding on how the fluidic field effect can be used with ISFGFET and under what conditions. We approach this problem by discussing the funda-

mental issues of the fluidic part and the double layer, formulate the model, thoroughly analyze the device, and then proceed to validate the proposed model with experiments.

When an oxide is immersed into an electrolyte solution, a native interface charge forms due to dissociation of hydroxyl groups at the surface. As a result, the surface attracts counter ions and repels the co-ions from the solution to neutralize the interface charge, and by doing so creates a double layer. The counter ions diffuse into the solution due to the thermal motion of ions and the diffuse layer potential decays into the solution exponentially. The length of the diffuse layer is described by the the ionic screening length (debye screening length) (see equation 2.12).

The Gouy-Chapman diffuse layer assumes point-like charges which for larger potentials leads to unrealistically high packing of ions at the surface. As the layer potential increases the charging and the concentration of ions must also increase. The exponential nature of the Gouy-Chapman diffuse layer charge potential relationship leads to significant charge pile up for potentials above one thermal voltage. Then the solution seizes to be dilute, which contradicts the original assumption. [69] Most practical considerations are interested in regions where this assumption fails. A widely accepted remedy for this is the Stern layer adjacent to the surface in series with the diffuse layer. This model is known as the Gouy-Chapman-Stern (GCS) model.

The Stern layer is a rigid layer of condensed ions where the ions cannot move normal to the surface and the ions cannot approach the surface closer than few nanometers, a distance limited by the ionic radius. [71] The zero charge density inside the layer implies a linear voltage drop across the layer. A constant Stern layer capacitance $18\mu F/cm^2$ is obtained assuming a 5Å charge separation with a dielectric constant of 10. Stern capacitance sets the upper limit on the system capacitance that would otherwise increase unrealistically without a limit. The differential double-layer capacitance C_{DL} can be expressed as a series capacitance of the diffuse layer capacitance C_{Gouy} and the Stern capacitance C_{Stern} and is given by $C_{DL} = (C_{Gouy}^{-1} + C_{Stern}^{-1})^{-1}$. As C_{Gouy} increases, the C_{DL} approaches the value of C_{Stern}.

The non-linear region in dilute solution formulation begins at potentials comparable to the thermal voltage of $\Psi_{DL} \approx kT/ze = 25mV$ (for monovalent ions). The Stern capacitance helps the overcharging of the diffuse layer but due to steric constraints it cannot stand a potential much larger than the steric limit. At larger potentials, the ions accumulating at the surface increase the length of the layer and extend it further into the solution [69]. One such formulation that allows the layer to extend is the modified Poisson-Boltzman model provided by Kilic et al. [69] The saturation in the charge pile up is achieved by incorporating a finite ion size in the model. This model is physically more realistic with one smoothly behaving layer as

opposed to the GCS model with physically unrealistic transitions between the rigid Stern layer and the diffuse layer. However, this model cannot account for specific ion adsorption, unlike the GCS model. It also ignores the permittivity variation of the solution with large electric fields. In the GCS model, this is accounted for.

Even though these models have their limitations, they can, with reasonable accuracy, predict the potential drop across the double layer. [71] If we consider the probing of the ionic screening layer, it is the region with modest charging that we are mostly interested in where the screening effect is mitigated. This was also observed in recent experiments by Jayant et al. [58]. In their experiments, maximum sensitivity in intrinsic DNA charge measurements was observed near the point of zero charge (PZC).

The early models of oxide surface sensitivity to bulk solution pH (pH_B) considered the Nernst equation. It predicted that a unit change in pH_B creates a potential shift at the oxide surface as $2.3kT/e$ [V/pH_B], where $kT/e \approx 25mV$ is the thermal voltage. This relation described by the Nernst equation is reasonable for glass electrodes but not for insulator interfaces that are not electric or ionic conductors. Modern theories rely on models originating from colloid chemistry where the site-dissociation model is combined with the double-layer theory. [39, 38, 78]

5.1.4 Compact Model of the ISFGFET

A simplified diagram of the ISFGFET and its equivalent circuit is shown in Figure 5.3. The system comprises the ISFGFET sensor previously described, but without the organic polymer functionalization on top of the oxide (Al_2O_3) layer. The electrolyte solution is modeled as a condensed Stern layer in series with a diffuse layer modeled with a Poisson-Boltzmann equation. The underlying FGFET structure consists of a SPICE modeled MOSFET that is coupled to the control (CG) and the sensing gate (SG). The corresponding potentials and capacitances are shown in Figure 5.3. The model is extensively described in (**II**) and the compact model repeated in Table 5.1 here is from (**III**).

The compact model is solved in a HSPICE sub-circuit block. The nonlinear equations (7) and (8) are solved using behavioral voltage sources. The FG and CG nodes are capacitively connected to n-type FET and are simulated using standard SPICE circuit elements. The block diagram of the macromodel is shown in Figure 5.3 b). There are six input nodes for the sub-circuit: control gate N1, reference electrode N2, drain N3, source N4, bulk N5, and a pH N100. The electrolyte pH has been included as a simple input node to allow simple simulation of the model for pH changes [78]. Using the model provided in Table 5.1, other parameters can be included similarly as a sub-circuit input node as well. The model specifies a user

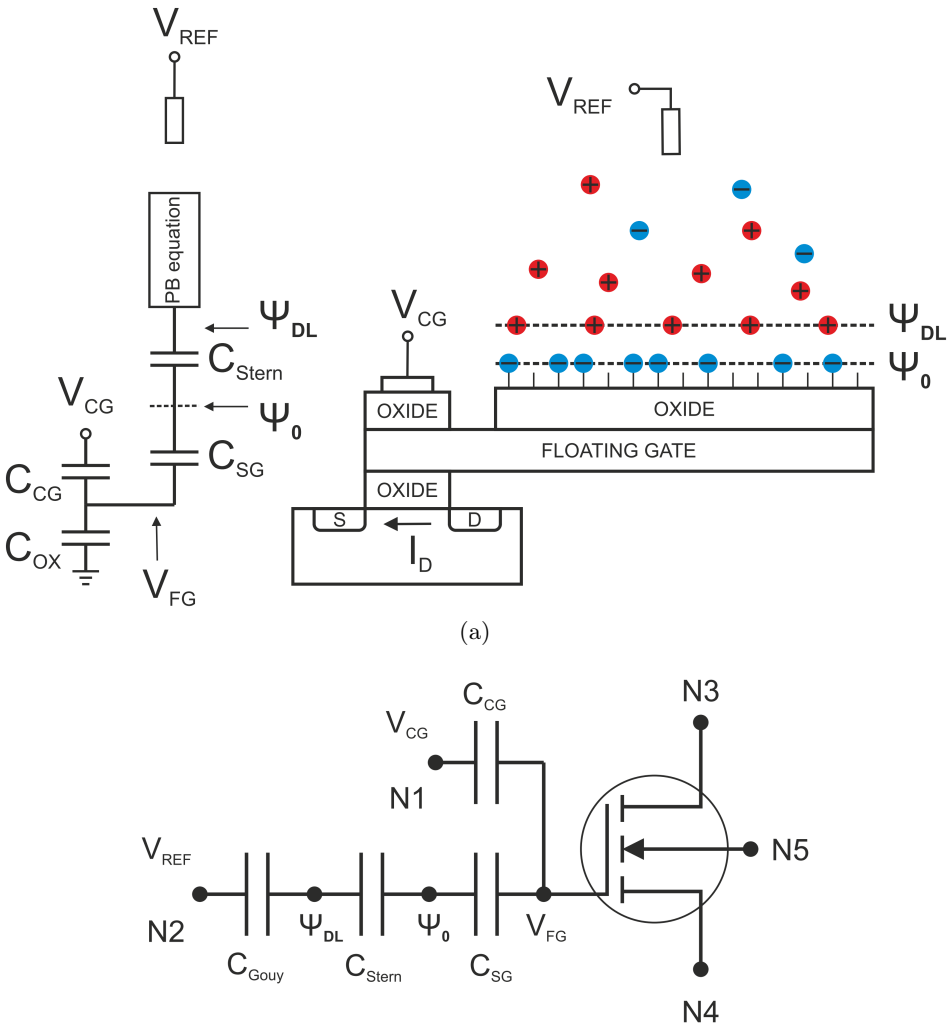

Figure 5.3: a) Simplified diagram of the ISFGFET (right) and its equivalent circuit (left) (**II**). The solution is modelled as a condensed Stern layer with its equivalent capacitance C_{Stern} and by the diffuse layer described by the Poisson-Boltzmann equation (PB-equation). The FGFET structure is modelled as a single gate nMOS with an added floating gate (FG), a control gate (CG) capacitor C_{CG}, and a sensing gate (SG) capacitor C_{SG}. These capacitors couple the V_{CG} and Ψ_0 to the FG. The channel oxide capacitance is C_{OX}. b) The equivalent macromodel of the ISFGFET where diffuse layer is expressed via a capacitor C_{Gouy} (**III**).

specific proprietary transistor model. In our case it is an n-MOS transistor comprising eight parallel transistor fingers and a CG capacitor. The sensor

has a pristine threshold voltage of 1 V at the FG. Both the CG and gate oxide capacitances are 0.13 pF.

The simulation results discussed below are either solved with Matlab combining SPICE simulations for the FET structure (**II**) or only using SPICE (**III**). Both approaches utilize the same theory and thus yield comparable results.

Table 5.1: Compact model equations

$S \cdot OH \overset{K_A}{\rightleftharpoons} S \cdot O^- + H_B^+(aq)$	(1)
$S \cdot OH_2^+ \overset{K_B}{\rightleftharpoons} S \cdot OH + H_B^+(aq)$	(2)
$\sigma_{SG} = C_{SG}(V_{FG} - \Psi_0)$	(3)
$\sigma_{DL} = C_{Stern}(\Psi_0 - \Psi_{DL})$	(4)
$V_{FG} = \frac{V_{CG}C_{CG} + \Psi_0 C_{SG}}{C_{TOT}} + \frac{Q}{C_{TOT}}$	(5)
$C_{TOT} = C_{CG} + C_{SG} + C_{OX}$	(6)
$\Psi_0 = V_{FG} + \frac{\sigma_0 - \sigma_{DL}}{C_{SG}}$	(7)
$\Psi_{DL} = \Psi_0 - \frac{\sigma_{DL}}{C_{stern}}$	(8)
$\sigma_0 = \frac{-e\Gamma}{1 + \frac{[H_B^+]}{Ka} exp\left(\frac{-e(\Psi_0 - V_{REF})}{kT}\right)} + \frac{e\Gamma}{1 + \frac{Kb}{[H_B^+]} exp\left(\frac{e(\Psi_0 - V_{REF})}{kT}\right)}$	(9)
$\sigma_{DL} = \frac{2e_w e_0 kT}{e\lambda_D} sinh\left(\frac{e(\Psi_{DL} - V_{REF})}{2kT}\right)$	(11)
$\lambda_D = \left(\frac{e_w e_0 kT}{2z^2 e^2 n_0}\right)^{1/2}$	(12)
$pK_a = -log_{10}(K_a), pKb = -log_{10}(K_b)$	(13)
$pH = -log_{10}([H^+])$	(14)

5.1.5 Simulation Results

The model was modified and incorporated for ISFGFET to predict its behavior under different surfaces and electrolyte solutions. The emphasis is given to how the surface potential Ψ_0 responds under different parameters on pH_B and V_{FG} and if CG initiated control can feasibly create the fluidic control. Unless otherwise stated all simulations consider the REF grounded, ionic strength as $c_0 = 10$ mM. The oxide thickness of the sensing gate is 10 nm. The results are gathered from (**II**) and (**III**).

The density of ionizable groups play an important part in the device behavior. In Figure 5.4 a) the relationship between the surface potential Ψ_0 and pH_B is shown when the number of ionizable groups is changed from an inert surface (no ionizable groups) to a surface with an abundance of these groups. The inert surface shows no pH sensitivity since there are no groups that can protonate or deprotonate. The high density case clearly shows a Nernstian response. Other factors such as double layer capacitance has an impact on the sensitivity, but as already noted by [38] the high density can compensate even high capacitance values. Between these two extremes can be found interesting surfaces that first exhibit pH_B sensitivity, but with increased/decreased pH levels, they behave as the surface was inert. This is a direct consequence of the surfaces having reduced buffering capacity.

The same effect can be studied by sweeping the oxide field strength with different ionizable groups densities and recording the Ψ_0 as shown in Figure 5.4 b). Now the surface with high density is practically unaffected by the varying field strength. Such a surface strongly counters, i.e., buffers the change in field strength by protonating or deprotonating. With high N_S only a small fraction of ionizable groups are required to respond to the varying field and thus can easily compensate changes in the V_{FG}. When N_S is decreased, the effect of varying V_{FG} has more of an impact on the surface potential. The surfaces with N_S equal to 0.1 or 0.2 in units of nm^{-2} have a gently sloping region near zero field strength. When the field strength increases, the slope steepens as a result of not having more ionizable groups to respond to the stimulus. Subsequently they behave like inert surfaces. The inert surface shows the biggest change in surface potential as it lacks buffering capacity altogether. The double-layer capacitance is large compared to C_{SG}. Therefore, in all cases the changes in Ψ_0 are small compared to the changes in V_{FG}.

The response can also be engineered via modifying the dissociation constants. In Figure 5.4 c) the effect of dissociation constant separation on Ψ_0 is simulated. The pK_A is kept constant but the pK_B is changed from 3 to 11. All the curves have similar shapes and changing the dissociation constant can be used to determine the pH_B sensitive region. The non-sensitive region widens upon increasing the pK separation, and when the pK values

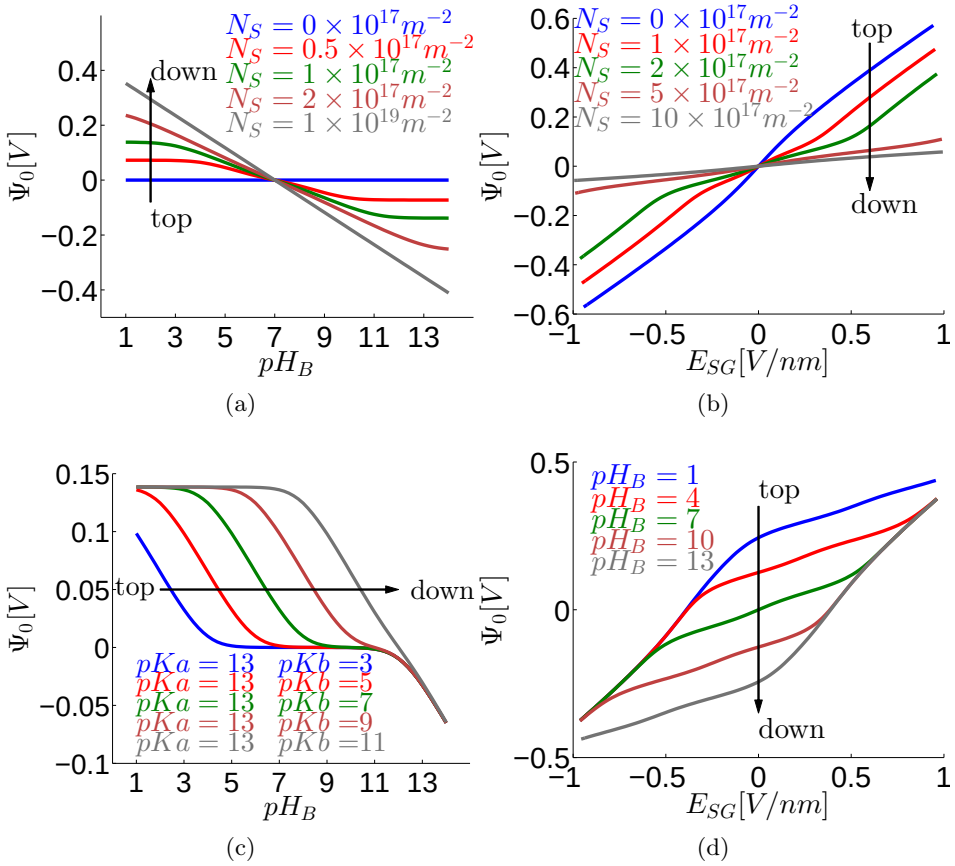

Figure 5.4: Relationship of surface potential Ψ_0 to pH_B and E_{SG} with varying ionizable site density and dissociation constants. The parameters used in the simulations unless otherwise stated were: $pK_A = 8$, $pK_B = 6$, $pH_B = 7$, $c_0 = 10$ mM, ϵ_r=9.3, d = 10 nm and $V_{REF} = 0$. In b) and d) V_{FG} was swept from -10 V to +10V resulting in the shown SG field strength $E_{SG} = (V_{FG} - \Psi_0)/d$. a) The surface pH_B sensitivity with different ionizable group densities. b) The relation between E_{SG} and Ψ_0 with different ionizable group densities. c) The effect of surface dissociation constant separation with $N_S = 1 \times 10^{17} m^{-2}$. d) The effect of pH_B on E_{SG} to Ψ_0 relationship with $Ns = 2 \times 10^{17} m^{-2}$. (**II**)

are sufficiently close together, there is no pH insensitive gap.

In Figure 5.4 d) the changes in Ψ_0 are simulated with different pH_B values and with sweeping insulator field strength. As in Figure 5.4 b) the flat part of the curves indicates the buffering region. Here a chemical modulation of the surface is achieved by simply changing the pH_B values. Decreasing pH_B creates more positive charges at the surface and shifts the buffering region

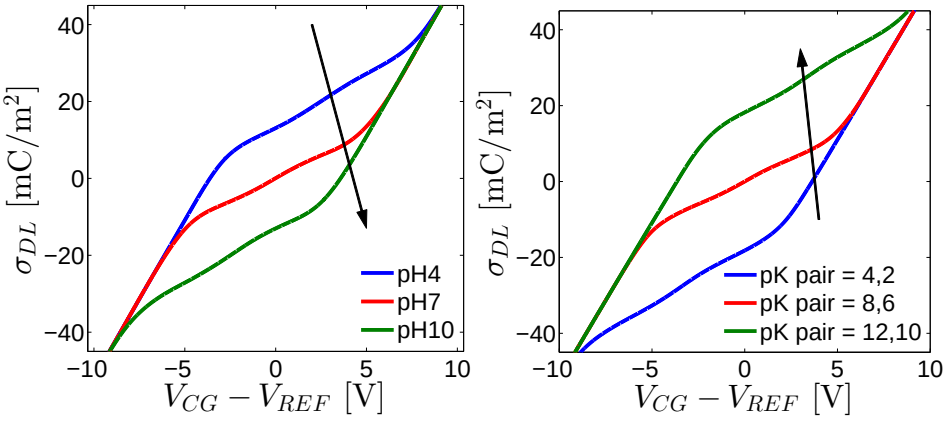

(a) (b)

Figure 5.5: Chemical and electrical tuning of the surface. a) Electrolyte pH is varied with $pK_A = 8$ and $pK_B = 6$. b) Surface dissociation constants are varied in pH = 7. In both cases the V_{REF} is considered grounded, $c_0 = 10$ mM and $N_S = 0.2\ nm^{-2}$. (**III**)

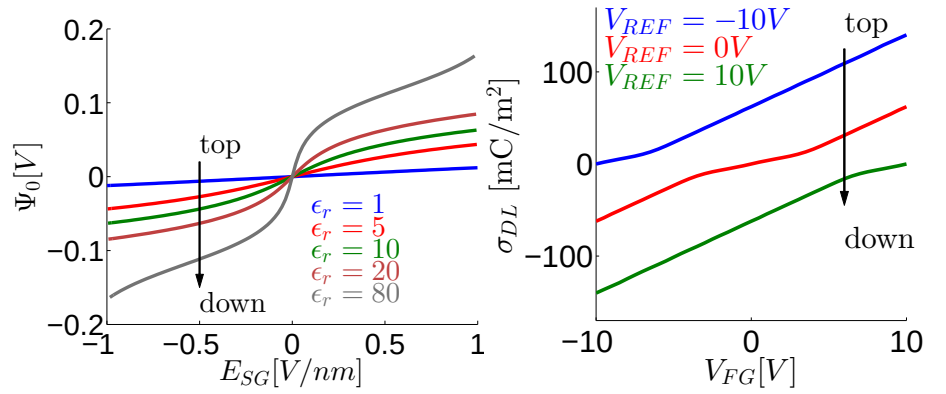

(a) (b)

Figure 5.6: a) The coupling strength increases (via increasing oxide ϵ_r) between the electrolyte solution and surface. The used simulation parameters were $N_S = 5 \times 10^{18} m^{-2}$, $pK_A = 9$ and $pK_B = 5$, $pH_B = 7$, $V_{REF} = 0$ and $c_0 = 10$ mM. b) The diffuse layer charge simulated with V_{REF} values of -10, 0 and 10 in units of V, with $N_S = 1 \times 10^{18} m^{-2}$, $pK_A = 8$, $pK_B = 6$ and $\epsilon_r = 9.3$. In all three cases, the double layer charging is determined by the potential across the electrolyte solution. (**II**)

to more positive field strengths.

The previous discussion was limited to surface potential simulations. The

electrofluidic gating also modulates the double layer screening. The double layer charge σ_{DL} can also be extracted from the simulations. It is possible to control the charging of the screening layer electrically via the field effect, by chemically adjusting the pH or by modifying the surface dissociation constants. The results are shown in Figure 5.5. In a) the chemical tuning using a pH variation is shown with the resulting change in charge. The change of pH changes the surface charging and thus the ionic screening layer. The same response can be achieved via surface modifications by engineering dissociation constants of the surface b). The analogous effect between the two are clear.

It is noteworthy to point out that here a CG is used to achieve the charging modulation by sweeping the CG potential V_{CG}. This sweeping creates an increased potential difference across the sensing gate oxide and the electrolyte. The simulated results indicate an intriguing interplay between electrical and chemical tuning of the double layer charging and between the electrolyte solution and interface parameters.

The ability of the field-effect control is limited by the dielectric breakdown of sensor oxides. Breakdown limits for common oxides Al_2O_3, SiO_2 and Si_3N_4 are 0.62 V/nm, 0.56 V/nm and 0.24 V/nm, respectively. [7] By increasing the dielectric constant, it is possible to increase the coupling of the electric field of the solution and thus amplify the effect of the electrofluidic gating. This is shown in Figure 5.6 a).

It is noteworthy to emphasize that it is the potential difference across the FG to REF that determines the charging conditions of the electrolyte. The result is shown in Figure 5.6 b) where the ionic screening layer charge σ_{DL} is plotted against V_{FG} with different V_{REF} values. This indicates that the interplay between RE and FG can be used to control the ionic screening layer charge and it can be set independently from the transistor operating point which is set by the V_{FG} and V_S.

The fluidic control via field effect seems plausible in semiconductor devices. For practical purposes many design compromises, however, need to be accounted for, i.e., material dielectric strength, dielectric constant, and thickness of the oxides as well as the underlying FET structure and the sensitivity of the device.

5.1.6 Verification of the ISFGFET model

The validity of the simulations were verified by comparing the simulations to earlier models (**III**) in comparable situations as well by comparing the measured ISFGFET transfer curves to corresponding simulations under different pH conditions (**II** and **III**). A well accepted model for pH-ISFETs is given by van Hal et al. [39, 38] This earlier model considers the electrolyte solution and the transistor as uncoupled and that the gate oxide is directly

Table 5.2: ISFET sensitivity comparison. Experiments for Al_2O_3 were conducted in pH range 1...13 @ 25 °C and for Ta_2O_5 in pH range 1...10 @ 25°C [102]. Both models were examined in pH range 1...14 in 1 M solution with Stern capacitance 18 $\mu F/cm^2$. All sensitivity values are in units of mV/pH$_B$.

Gate material	ISFET model [39]	ISFGFET macromodel	ISFET measured [102]	ISFGFET measured [63]
Al_2O_3	53.0	53.2	53.2	50.9
Ta_2O_5	58.5	58.6	59.4	

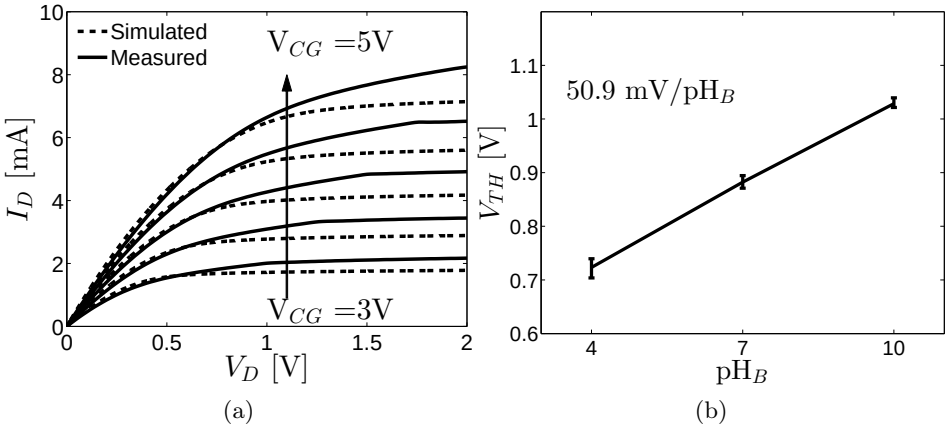

(a) (b)

Figure 5.7: a) Transistor transfer characteristics. I_D vs. V_D with V_{CG} values of 3 V to 5 V. $V_{FG} \approx 1/2 \times V_{CG}$. b) ISFGFET pH_B sensitivity characterization in pH_B values of 4, 7, and 10. (**II** and **III**)

the sensing gate. Additionally, the double layer is assumed as a single capacitance from which the surface potential is simply computed as $\Psi_0 = \sigma_0/C_{DL}$. These simplifications are not followed here and the Stern layer and diffuse layer are treated separately, which allows the computation of both surface charging and the ionic screening layer charge.

The pH response was computed with Al_2O_3 and Ta_2O_5 surfaces using both models. The results are collected in Table 5.2. The pH_B sensitivities between the models with Al_2O_3 and Ta_2O_5 surfaces are in agreement. The ISFGFET device has a floating node which is surrounded by a capacitive network. Since the node is floating a small part of change in the surface charge is seen in it. This creates a small difference between the sensitivities shown in Table 5.2. Moreover, reported measurement results using commercial Sentron 1090 Al_2O_3 ISFET and a Ta_2O_5 gate ISFET [102] show good

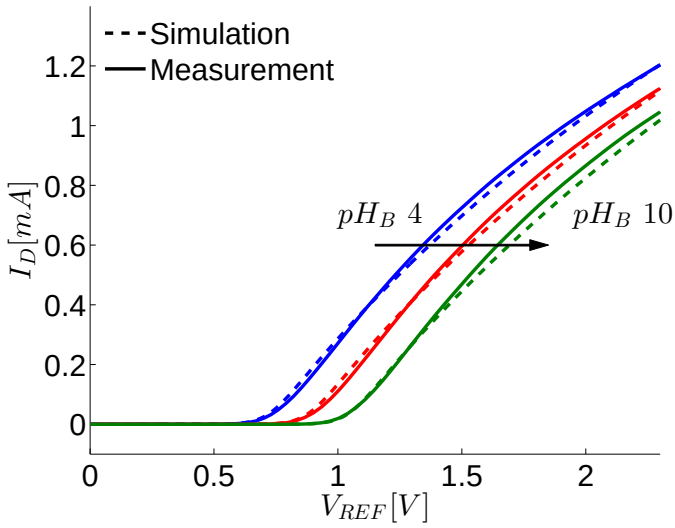

Figure 5.8: ISFET-mode transfer characteristics and pH sensitivity comparison between model and experiments in pH_B values of 4, 7 and 10. V_D is 0.1 V. (**II** and **III**)

agreement with the computations as well measured values of the ISFGFET shown in Figure 5.7 b). In a) the device transfer curves are shown under electrical testing indicating that the underlying transistor model is generally correct, but requires a small correction factor. The transfer curve analysis has been treated with more details in [63] (**III**).

Figure 5.8 compares the simulation results to measured transfer curves under chemical sensing indicating a close match between the two. The model is able to predict not only the pH_B sensitivity but also to match the transfer curves in their absolute values of V_{REF} and I_D. Moreover, the transconductance reduction usually observed in ISFETs [44] is negligible. This result was found by simulating the MOSFET model and by considering the FG as the gate without the chemical part or the capacitive network and by comparing it to the measured results with the CG left floating. The reduction is negligible due to the large C_{SG}. Additionally, no significant threshold variations were observed that are common in unmodified CMOS ISFETs due to the trapped charge in the passivation layer [77].

5.2 Design of the General Sensing System

Sensors that could be operated in a broad range of settings especially in remote and poor resource locations with minimal user training need to be inexpensive and simple to use. A clear benefit could be achieved if the sensor

(a)

Figure 5.9: The sensing system consisting of an 1) the custom sensing platform; 2) the hand-held readout device; 3) cable connecting the platform to the reader and; 4) a smart phone for data plotting and storage. (**V**)

could be coupled to a cloud allowing simple sharing and processing of data [88]. For these purposes a device that can access a mobile network and that can make a variety of measurements at low cost is a must. This problem was approached by designing a hand held multiplexed potentiometric sensing system. The system allows sensing at remote locations by using a mobile phone as control and storage device and also allowing an access to a mobile network. The developed general all electrical multiplexed sensing system (GEMSS) is based on a portable readout device, a mobile phone and a custom chemical sensing platform. The components of the system are shown in Figure 5.9. The chemical sensing platform relying on low-cost electronic manufacturing processes is coupled to a hand held readout device. The device connects to a smartphone using a wireless connection.

The block diagram of the designed chemical sensor readout device is shown in Figure 5.10. The system comprises (i) a two-channel analog front end that utilizes a constant-voltage-constant-current (CVCC) bias circuitry which ensures a direct relation between changes at the sensing layer voltage and output; (ii) a four channel 16-bit ADC which measures the output of two sensors; (iii) the voltage from a temperature measuring circuit implemented as a voltage divider where a PT1000 sensor element is placed at the custom

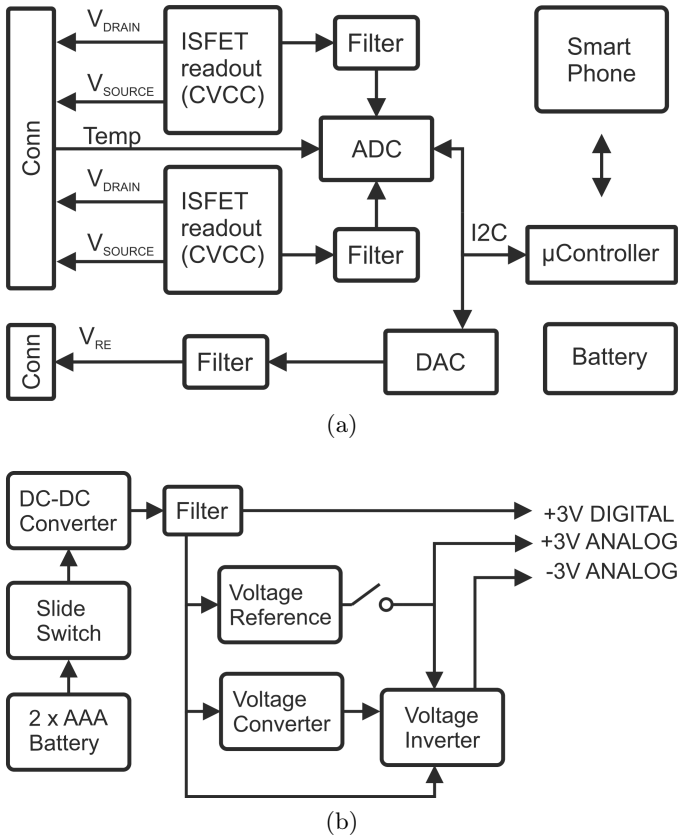

Figure 5.10: a) Block diagram of the readout device. b) Power generation for the readout device from battery. (**V**)

sensor platform; (iv) single channel 16-bit DAC that provides bias to the reference electrode; (v) DC-DC converter that keeps the voltage from the pair of AAA batteries constant; (vi) low noise voltage reference for bias circuit that drive the sensors for precision analog signal measurements; (vii) a voltage converter that inverts a positive signal to a negative signal; (viii) the converter is coupled with an inverter that draws negative supply from a noisy converter signal and inverts the stable positive reference signal; (ix) an analog switch that is used to couple/decouple the analog front end (AFE); and (x) a microcontroller unit that controls the data acquisition and transmission to a smartphone using low energy Bluetooth.

The power generation for the system is depicted in Figure 5.10 b). The system utilizes a mechanical switch that allows full decoupling of batteries, thus maximizing the lifetime of the batteries during a possibly long idle time between measurements. A precision voltage source is used to generate both positive and negative references for the constant current sources. The

negative source is implemented using a simple inverting op-amp with a high power supply rejection ratio. The op-amp powers negative supply from a fairly noisy negative voltage converter.

The biasing circuitry plays an important part of the GEMSS. It buffers the sensors output before being filtered and converted to a digital form and ensures a direct relationship between measured potential changes and the changes in chemical potential. The sensing transistors and the biasing circuit are protected from improper connections when a reference electrode is not used. This is done using an analog switch controlled by the software by decoupling all bias related power sources when the measurement is off and the circuit is not electrically closed.

5.2.1 Device Operation and Performance

The designed bias circuit ensures a linear relationship between the transistor gate and the measured output. The system power consumption was minimized. The total current consumption of the device from 3 V battery is less than 6 mA with a 10 Hz sample rate and data transmission on. With the two AAA batteries the expected lifetime is 300 h before new batteries are required.

The designed extended-gate ISFET sensing principle is analogous to potentiometric measurements [52, 15]. In an electrochemical cell exists many interfaces and across each of them exists a potential difference. The total cell potential is the sum of these potentials. [113] All constant potentials can be lumped into a single parameter, simplifying the expressions for the cell potential

$$V_{cell} = V_{cell}^{0} + \frac{RT}{z_i F} \ln(a_i + K_{i,j} a_j^{z_i/z_j} + L) \tag{5.6}$$

where a is the activity (i for the primary ion and j for the interfering ion), $K_{i,j}$ is the selectivity coefficient, L is included for the limit of detection and z is the valence of a spesific ion. R,T and F are the gas constant, temperature, and the Faraday constant respectively. [15]

In the EG-ISFET configuration, the MOSFET gate is not removed and thus the threshold voltage as such is in series with the chemical potential

$$V_{th}^{isfet} = V_{th}^{mosfet} + V_{cell} \tag{5.7}$$

The cell potential is (ideally) the only parameter in the system that produces a change in potential according to the target concentration in the sample. Thus, the relationship between changes in V_{th}^{isfet} ISFET (with n-type MOSFET) and in the cell potential reads

$$\Delta V_{chem} = -\Delta V_{th}^{isfet} \tag{5.8}$$

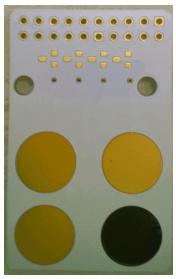

(a)

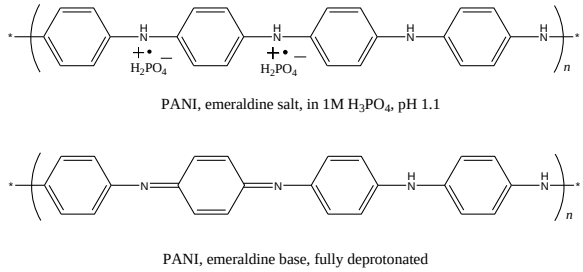

(b)

Figure 5.11: a) An example of the sensing platform with one functionalized sensing element. The top two rows are through holes for the connector that provides bias for transistors. Below are the connector soldering pads for four SOT-23 case transistors, one for each sensing element. (**IV**) b) Fully protonated (top) and fully deprotonated (bottom) emeraldine form of PANI used in (**IV**).

V_{chem} is defined as the chemically sensitive part of the electrochemical cell potential.

5.3 Chemical Sensing with EGISFET

The main objective in (**IV**) was to validate the proposed sensor concept that relies on existing electrical manufacturing processes and commercial discrete transistors. We compared the designed sensing platform to routinely used open circuit measurements (OCP) using a conventional glassy carbon (GC) electrode. We investigated the pH sensitivity, pH time response, and the drift. Additionally the presence of transconductance reduction, which is commonly observed in extended gate pH-ISFETs with oxide sensing layers, was measured. The array platform used for this study is shown in Figure 5.11.

The applicability of the sensing platform after successful demonstration of the principle was tested using ion-selective membranes in the configuration shown in the Figure 5.12 and the GEMSS. The conventional ion-selective-electrodes (ISE) are commonly bulky and fragile and rely on membranes passing though specific ions from the sample solution to the internal filling solution. [82] A more advanced version is solid-state electrodes where no internal filling solutions are used, but a selective membrane is deposited on the electrode surface. [15] Commonly a glassy carbon electrode is used which is expensive, bulky, and not suitable for disposable sensing or outside laboratory use. A common problem with solid state electrodes is the sig-

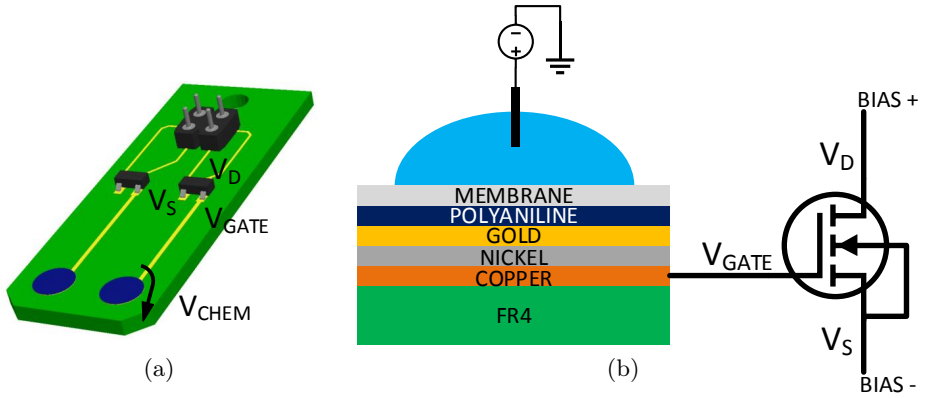

(a) (b)

Figure 5.12: a) Illustration of an two channel platform and b) a corresponding schematical illustration of the sensor (**V**).

nificant drift if no transducing layer is used. [16] To test the applicability, a potassium selective membrane was selected using PANI-DNNSA as the intermediate ion-to-electron transducing layer.

The membrane can be deposited by casting it onto the sensor surface. The procedure is general and the sensor can be extended to various different analytes such as Sodium (Na+), Calcium (Ca++), Copper (Cu++) and Lead (Pb++) using the same platform and depositing techniques. The proposed approach additionally allows other substrate materials including flexible plastic substrates. It is expected that the simple fabrication procedure makes it easier for others to design and fabricate FET based sensors for potentiometric applications.

5.3.1 Performance of the Chemical Sensing Platform

In extended gate ISFETs with oxide membranes, a capacitor is formed in series with the transistor gate oxide when an insulator, commonly oxide, is used as a sensing layer. This effectively reduces the device transconductance [44, 83]. We investigated how this reduction is present with the extended gate in the platform designed with PANI-H_2PO_4 deposited on gold. We simultaneously probed V_{OUT}, V_G, and V_{REF}. The negligible difference in the slopes of the curves imply that the voltage division does not have any practical influence on the device transconductance. This is shown in Figure 5.13 a).

The potential of polyaniline is pH dependent and it decreases as the pH increases. Polyaniline and its substituted derivatives have different pH sensitivities ranging from slightly super Nernstian dependencies to almost non-responsive pH sensitivities. [76] For the construction of biosensors, the

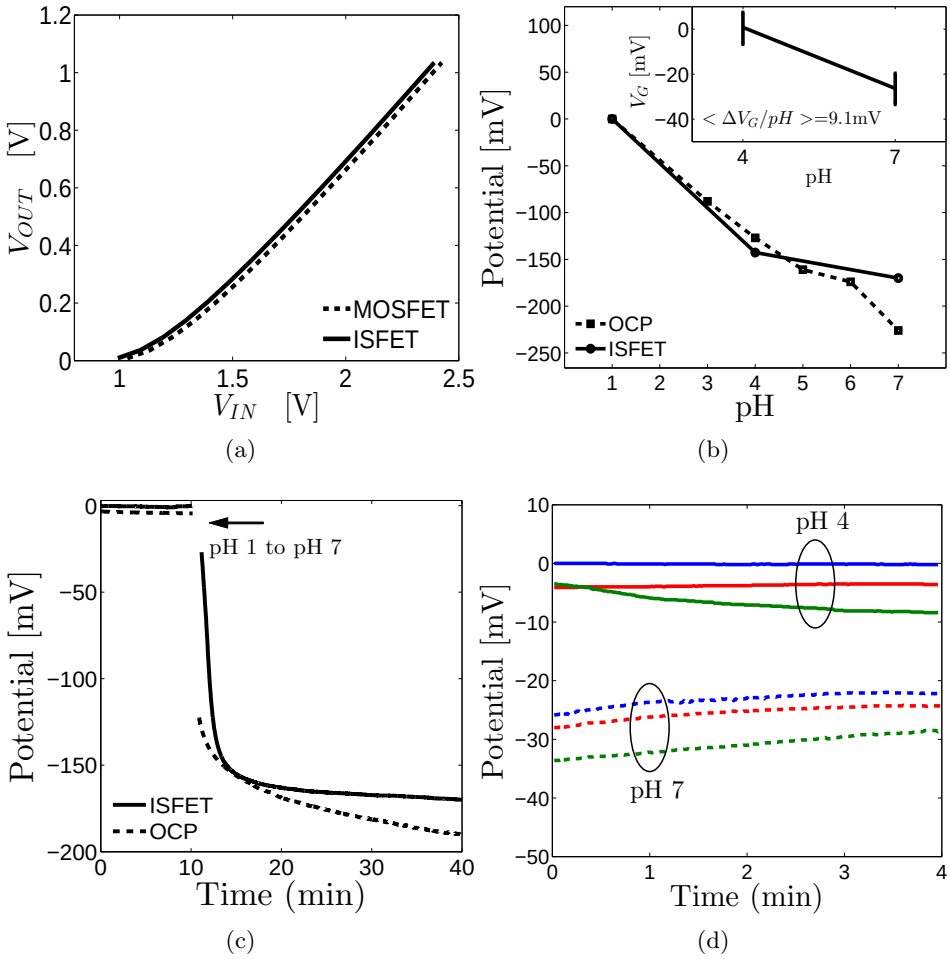

Figure 5.13: a) Transfer characteristics of the sensor measured by sweeping the RE voltage. The results are plotted showing the transfer characteristics of the MOSFET only and the ISFET configuration. b) pH sensitivity comparison of the developed EG-ISFET platform and OCP with GC electrode and c) the pH time response comparison. Initial drift when the platform array is immersed into the solution. All figures adapted from (**IV**).

suppressed pH sensitivity is important according to the theory of biosensors. [99] The pH sensitivity depends on the size of the acid anion and the substituent.[76] When polyaniline is fully deprotonated, the protons are removed from the backbone of PANI and counter-ions are released to the solution. PANI-H_2PO_4 exhibits low pH sensitivity in the pH range where most bioassays operate, indicating a possibility of constructing a simple disposable biosensor based on existing electronic manufacturing processes. The

pH sensitivity of the ISFET platform was compared to OCP measurements with glassy carbon electrodes under the same reactions. This is shown in Figure 5.13 b). The sensitivities are in good agreement between pH 1 to pH 4. In the the pH range from 4 to 7, the ISFET has more suppressed sensitivity. We attribute this beneficial feature in biosensor construction to the different substrate onto which PANI is drop-casted. The work functions of carbon and gold are different making the interfacial behavior between the substrate and PANI different. Thus, the PANI pH sensitivity is different in OCP and ISFET measurements. Moreover, the PANI adhesion on the surface might change between different surfaces and its impact on pH sensitivity is not known.

The pH time response of the PANI functionalized sensor was investigated to compare the new ISFET platforms response time compared to the well known glassy carbon electrode under OCP. The response was recorded when a pH 1 (1 M HCl) solution was changed to a pH 7 0.05 M phosphate buffer solution. Upon pH change, the polyaniline deprotonates resulting in decreased output voltage. The OCP and ISFET have similar fast response times indicating well defined interfacial behavior. This is shown in Figure 5.13 c).

The oxide based ISFETs are known to have a strong monotonic drift after immersed in a solution [50]. The drift of the ISFET array platform was tested in pH 4 and pH 7 solutions by immersing neutral state PANI sensing pads to the solution and recording the output directly after the immersion. No systematic drifts are observed as shown in Figure 5.13 d). Small drift properties have also been reported in [115].

5.3.2 Performance of the Solid Contact K^+ Electrode

The properties of the sensing platform were tested in terms of stability, sensitivity, and dynamic range. The GEMSS system was compared using the developed chemical sensing platform with a conventional OCP voltmeter and the developed GEMSS that employs the FET as an impedance transforming element near the chemically sensitive area. This creates a practically noise free environment, a common problem in OCP. Moreover, we employed a new transducing material the PANI-DNNSA that can be deposited via a simple one step casting.

The stability of the sensors were tested with three different membrane compositions. These are explained in the materials sections. A positive drift in the OCP potential are known to indicate the presence of a water layer between the selective membrane and the solid contact [27, 75]. Typical time evolutions of the platforms are shown in Figure 5.14. From the results it can be seen that the new employed hydrofobic PANI-DNNSA transducing layer successfully eliminates this layer where the coated electrode configuration

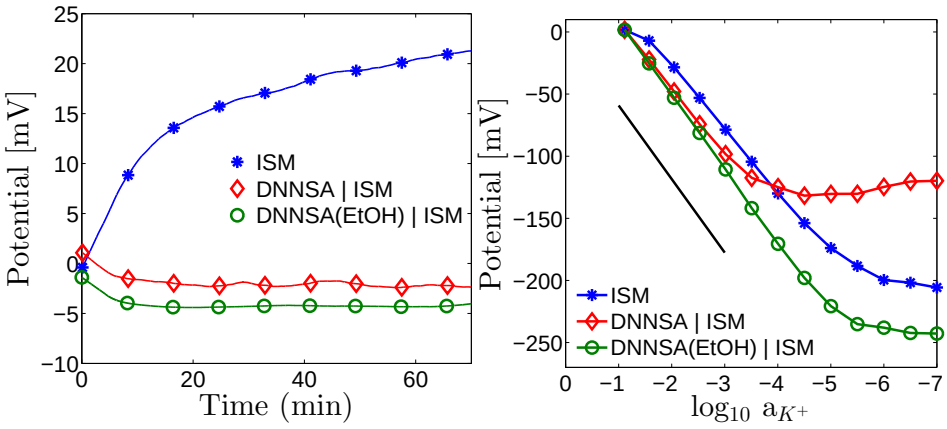

(a) ISFET (b) ISFET

Figure 5.14: Different membrane composition comparisons of the ISFETs. All measurements are done in KCl solutions. The drift is measured in 0.1 M KCl and calibration curves are obtained by half decade step dilutions starting from 0.1 M KCl. a) drift b) end point calibration

does not reach stable potential. The sensor shows practically ideal drift characteristics.

After successful water layer elimination, the sensors were characterized via calibration curves. The sensor with the EtOH treated transducing layer routinely showed a dynamic range up to four orders of magnitude and always well above three orders. A similar selective membrane with molybdenum sulfide (MoS2) nanoflowers [120] shows a slightly smaller dynamic range under conventional OCP using glassy carbon electrodes. Without EtOH treating the PANI-DNNSA, the dynamic range is clearly reduced. We attribute this to the solubility of the solid contact which partly dissolves into the ion-selective membrane.

The trace calibration curves shown in Figure 5.15 a) and b) indicate the absence of the water layer with good potential stability throughout the entire concentration range of the titration. Moreover, each step is accompanied by a stepwise decrease of the potential with minimal stabilization time after the concentration change. Such behavior is common to electrodes with hydrophobic contact. [41] The sensing platform was also calibrated similarly in the presence of interfering ions. Even in the presence of a high concentration of interfering ions, the electrodes do not show a diminished limit of detection and the sensors are fully stable and exhibit short response times.

The end point calibration curves are shown in Figure 5.15 c). The ISFETs show near Nernstian responses with a linear dynamic range with almost four orders of magnitude. An average of four measurements for each step is

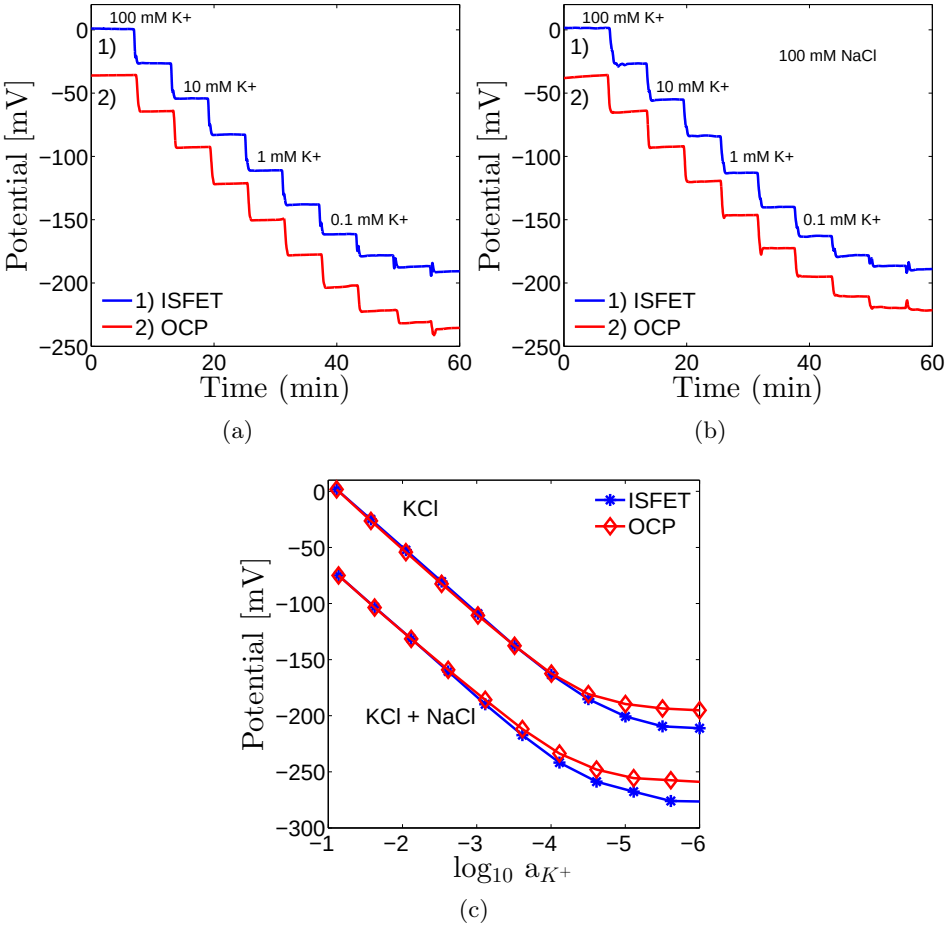

Figure 5.15: Trace calibration curves for both OCP and ISFET configuration with b) and without interfering ions a) and end point calibration curves collected in c) with an average of four measurements for each case.

shown. ISFET configuration systematically shows slightly improved limit of detection.

Chapter 6

Conclusion

Biosensing markets are emerging as a significant industry with repeating annual growth. Chronic and lifestyle associated diseases and aging populations are driving the growth of point-of-care (POC) markets and global environmental monitoring is gaining significant share due to increasing pollution and global population. [33, 26] For creating portable and low-cost devices that could be utilized out of laboratory settings, electrical sensing is a promising alternative. Transistor based sensors are inherently miniature and have high parallel sensing abilities. The obtained signal is directly in electrical form, which allows convenient data processing and sharing.

In this thesis, field-effect based sensing was studied both theoretically and experimentally. It investigates a new type of ISFET derivative, modified with an additional control gate, called the ISFGFET (**I**, **II** and **III**). This multipurpose control gate can be used to bias the transistor as well as serve as a source for field-effect control of the electrolyte solution. In publication I, the emphasis was on polymer functionalization of the device. The device proved to behave similarly as a comparison measurement done with open circuit potentiometry and as qualitatively explained through the developed model. The functionalization can be achieved via a simple drop-casting. The used functionalization has been shown to be promising for sensitive as an ion-electron tranducer as well as for immunosensing with direct electron transfer between the surface and the reaction product, and the functionalization creates low pH sensitivity which is a necessity in biosensor design [124]. In addition the used polymer can be thiolated [13] pawing the way for DNA sensor with thiolated probe DNA attachment. The reference electrode free operation was verified and the plausibility for such operation was found. However, leaving sensing gate and electrolyte solution without a stable and well defined potential the gate serves as an miniature antenna and becomes highly charge sensitive and in practical situations can easily generate noisy signals. The sensor, however, can be easily used by using the

reference electrode and as such can be highly beneficial with and without using the control gate (second input gate) as thoroughly explored in (**II** and **III**)

The ISFGFET properties were studied with a oxide sensing layer in pH sensing applications (**II** and **III**). A new model was developed that did not make the same simplifying assumptions as earlier models. This revealed that the device can be used for field-effect control of the electrolyte solution. Such a property cannot be predicted with earlier models nor is it possible with conventional ISFET structures. It was found that the property is plausible with CMOS devices. A trade off with sensitivities, however, needs to be considered. The two input gates, both capacitively coupled to the common floating gates, create a weighing factor reducing the coupling strength of either one of the gates. This sensitivity reduction and the strength for fluidic control are interrelated. Additionally, the high buffering capacity necessary for pH sensing needs to be reduced if a fluidic control is desired, as the high density of ionizable groups can easily counter all attempts for electrofluidic gating. This property is envisioned to be beneficial in new detection schemes where the isoelectric point can be controlled, for enhancing sensing probe immobilization on the surface, or when charged macromolecule transport is desired in biosensing applications. However, these different applications require application specific design efforts. The model was verified through experiments and translated into an intuitive macromodel that can be efficiently computed and include complicated circuit design as part of the CMOS design flow. Moreover, a robust analysis of parasitic capacitances is viable with the new model and the addition of temperature and drift effects can be included further extending understanding of field-effect sensors.

Although CMOS based solutions have great parallel sensing abilities, the common problems with encapsulation have limited their widespread use. For many sensing applications such vast parallel computations are not necessary. For these purposes, a low-cost platform based on discrete components and existing manufacturing processes was developed (**IV** and **V**). The designed platform allows simple surface modifications and multiplexed detection. This sensor was functionalized with polyaniline and its operation was characterized in pH solutions in terms of sensitivity, response time, drift and whether the sensors exhibit a transconductance reduction as commonly observed with pH ISFETs. The study revealed the sensing platform has comparable performance and was achieved at much lower costs than traditional laboratory equipment. A full sensing system solution was designed that allows a battery operated hand-held device to be used for reading the output of the chemical sensing platform. All operations are controlled via a mobile phone including measurement initiation, data transfer, and data storage. The design of the system was presented in detail. The system provides a linear response between the chemical potential and the output of the biasing circuit. This

device was characterized by detection of potassium with and without interfering ions. Finally, the applicability of the low-cost system was tested in the detection of blood electrolytes by determining the amount of potassium in the blood serum. The results indicate the possibility to use the low-cost system for biologically relevant measurements. Moreover, a one step calibration method was employed for an easier user experience.

The developed general electrical sensing system (GEMSS) is based on existing commercial electrical components and manufacturing processes. This allows the sensing platform to be produced at a cost of 0.3 EUR quoted for 1000 units excluding the cost of chemically sensitive materials. The portable and wireless readout device was not cost optimized, but a similar design could be pushed well below 100 EUR excluding the phone. The system can be utilized in very diverse settings and for different applications. The performance is comparable and in terms of detection limit and noise properties better than the more bulky and expensive electrodes. Moreover, the used conducting polymers allow the sensing system to be modified towards enzymatic reactions and antibody/antigen interactions or DNA detection. Additionally, the platform is not limited to conducting polymer functionalization, but for example, the gold surface could be directly functionalized with oligonucleotide probes or proteins (antigens or antibodies) or modified with other mediator layers such as graphene. The data is sent wirelessly to a smartphone allowing direct access to data sharing and storing via mobile networks. The developed sensing system provides an important step towards miniaturized systems for various targets in (bio)chemical sensing in situ.

Bibliography

[1] Abi, A. and Ferapontova, E. E. "Unmediated by DNA Electron Transfer in Redox-Labeled DNA Duplexes End-Tethered to Gold Electrodes". In: *Journal of the American Chemical Society* 134 (2012), pp. 14499–14507.

[2] Abramova, N., Ipatov, A., Levichev, S., and Bratov, A. "Integrated multi-sensor chip with photocured polymer membranes containing copolymerised plasticizer for direct pH, potassium, sodium and chloride ions determination in blood serum". In: *Talanta* 79 (2009). 15th International Conference on Flow Injection Analysis, Nagoya, Japan, 28 September - 3 October 2008, pp. 984 –989.

[3] Arya, S. K., Wong, C. C., Jeon, Y. J., Bansal, T., and Park, M. K. "Advances in Complementary Metal Oxide Semiconductor Based Integrated Biosensor Arrays". In: *Chemical Reviews* 115 (2015), pp. 5116–5158.

[4] Barbaro, M., Caboni, A., Loi, D., Lai, S., Homsy, A., Wal, P. van der, and Rooij, N. de. "Label-free, direct DNA detection by means of a standard CMOS electronic chip". In: *Sensors and Actuators B: Chemical* 171,172 (2012), pp. 148 –154.

[5] Barbaro, M., Bonfiglio, A., and Raffo, L. "A charge-modulated FET for detection of biomolecular processes: conception, modeling, and simulation". In: *IEEE Transactions on Electron Devices* 53 (2006), pp. 158–166.

[6] Barbaro, M., Bonfiglio, A., Raffo, L., Alessandrini, A., Facci, P., and Barak, I. "Fully electronic DNA hybridization detection by a standard CMOS biochip". In: *Sensors and Actuators B: Chemical* 118 (2006), pp. 41 –46.

[7] Bartzsch, H., Glös, D., Frach, P., Gittner, M., Schultheis, E., Brode, W., and Hartung, J. "Electrical insulation properties of sputter-deposited SiO2, Si3N4 and Al2O3 films at room temperature and 400 C". In: *physica status solidi (a)* 206 (2009), pp. 514–519.

[8] Bausells, J, Carrabina, J, Errachid, A, and Merlos, A. "Ion-sensitive field-effect transistors fabricated in a commercial CMOS technology". In: *Sensors and Actuators B: Chemical* 57 (1999), pp. 56 –62.

[9] Bergveld, P. "Development of an Ion-Sensitive Solid-State Device for Neurophysiological Measurements". In: *IEEE Transactions on Biomedical Engineering* BME-17 (1970), pp. 70–71.

[10] Bergveld, P. "ISFET, Theory and Practice". In: *IEEE Sensor Conference Toronto* (2003).

[11] Bergveld, P. "Thirty years of ISFETOLOGY: What happened in the past 30 years and what may happen in the next 30 years". In: *Sensors and Actuators B: Chemical* 88 (2003), pp. 1 –20.

[12] Blin, A., Cisse, I., and Bockelmann, U. "Electronic hybridization detection in microarray format and DNA genotyping". In: *Scientific Reports* (2014).

[13] Blomquist, M., Bobacka, J., Ivaska, A., and Levon, K. "Electrochemical and spectroscopic study on thiolation of polyaniline". In: *Electrochimica Acta* 90 (2013), pp. 604 –614.

[14] Bobacka, J., Ivaska, A., and Lewenstam, A. "Potentiometric Ion Sensors Based on Conducting Polymers". In: *Electroanalysis* 15 (2003), pp. 366–374.

[15] Bobacka, J., Ivaska, A., and Lewenstam, A. "Potentiometric Ion Sensors". In: *Chemical Reviews* 108 (2008), pp. 329–351.

[16] Boeva, Z. A. and Lindfors, T. "Few-layer graphene and polyaniline composite as ion-to-electron transducer in silicone rubber solid-contact ion-selective electrodes". In: *Sensors and Actuators B: Chemical* 224 (2016), pp. 624 –631.

[17] Boeva, Z. A., Milakin, K. A., Pesonen, M., Ozerin, A. N., Sergeyev, V. G., and Lindfors, T. "Dispersible composites of exfoliated graphite and polyaniline with improved electrochemical behaviour for solid-state chemical sensor applications". In: *RSC Adv.* 4 (86 2014), pp. 46340–46350.

[18] Bousse, L., Rooij, N. F. D., and Bergveld, P. "Operation of chemically sensitive field-effect sensors as a function of the insulator-electrolyte interface". In: *IEEE Transactions on Electron Devices* 30 (1983), pp. 1263–1270.

[19] Caras, S. and Janata, J. "Field effect transistor sensitive to penicillin". In: *Analytical Chemistry* 52 (1980), pp. 1935–1937.

[20] Cattrall, R. W. and Freiser, H. "Coated wire ion-selective electrodes". In: *Analytical Chemistry* 43 (1971), pp. 1905–1906.

[21] Chen, S. “Electronic Sensors Based on Nanostructured Field-Effect Devices”. PhD thesis. Uppsala Universitet, 2013.

[22] Cui, Y. and Lieber, C. M. “Functional Nanoscale Electronic Devices Assembled Using Silicon Nanowire Building Blocks”. In: *Science* 291 (2001), pp. 851–853.

[23] Deen, M. J., Shinwari, M. W., Ranuarez, J. C., and Landheer, D. “Noise considerations in field-effect biosensors”. In: *Journal of Applied Physics* 100, 074703 (2006).

[24] Dhand, C., Das, M., Datta, M., and Malhotra, B. “Recent advances in polyaniline based biosensors”. In: *Biosensors and Bioelectronics* 26 (2011), pp. 2811 –2821.

[25] Dzyadevych, S. V., Soldatkin, A. P., El’skaya, A. V., Martelet, C., and Jaffrezic-Renault, N. “Enzyme biosensors based on ion-selective field-effect transistors”. In: *Analytica Chimica Acta* 568 (2006), pp. 248 – 258.

[26] *Environmental Monitoring Market by Product, Application and by Region - Global Trends and Forecasts to 2020*. Markets and Markets, 2015.

[27] Fibbioli, M., Morf, W. E., Badertscher, M., Rooij, N. F. de, and Pretsch, E. “Potential Drifts of Solid-Contacted Ion-Selective Electrodes Due to Zero-Current Ion Fluxes Through the Sensor Membrane”. In: *Electroanalysis* 12 (2000), pp. 1286–1292.

[28] Fixe, F, Branz, H., Louro, N, Chu, V, Prazeres, D., and Cond, J. “Immobilization and hybridization by single sub-millisecond electric field pulses, for pixel-addressed DNA microarrays”. In: *Biosensors and Bioelectronics* 19 (2004), pp. 1591 –1597.

[29] Fritz, J., Cooper, E. B., Gaudet, S., Sorger, P. K., and Manalis, S. R. “Electronic detection of DNA by its intrinsic molecular charge”. In: *Proceedings of the National Academy of Sciences* 99 (2002), pp. 14142–14146.

[30] Gao, N., Zhou, W., Jiang, X., Hong, G., Fu, T.-M., and Lieber, C. M. “General Strategy for Biodetection in High Ionic Strength Solutions Using Transistor-Based Nanoelectronic Sensors”. In: *Nano Letters* 15 (2015), pp. 2143–2148.

[31] Georgiou, P. and Toumazou, C. “ISFET characteristics in CMOS and their application to weak inversion operation”. In: *Sensors and Actuators B: Chemical* 143 (2009), pp. 211 –217.

[32] Ghowsi, K. and Gale, R. J. “Field effect electroosmosis”. In: *Journal of Chromatography A* 559 (1991). Third International Symposium on High Performance Capillary Electrophoresis, pp. 95 –101.

[33] *Global Market Study on Biosensor: Asia-Pacific to Witness Highest Growth by 2020*. Persistence Market Research, 2014.

[34] Goda, T., Singi, A. B., Maeda, Y., Matsumoto, A., Torimura, M., Aoki, H., and Miyahara, Y. "Label-Free Potentiometry for Detecting DNA Hybridization Using Peptide Nucleic Acid and DNA Probes". In: *Sensors* 13 (2013), p. 2267.

[35] Goykhman, I., Korbakov, N., Bartic, C., Borghs, G., Spira, M. E., Shappir, J., and Yitzchaik, S. "Direct Detection of Molecular Biorecognition by Dipole Sensing Mechanism". In: *Journal of the American Chemical Society* 131 (2009), pp. 4788–4794.

[36] Grieshaber, D., MacKenzie, R., Vörös, J., and Reimhult, E. "Electrochemical Biosensors - Sensor Principles and Architectures". In: *Sensors* 8 (2008).

[37] Gubala, V., Harris, L. F., Ricco, A. J., Tan, M. X., and Williams, D. E. "Point of Care Diagnostics: Status and Future". In: *Analytical Chemistry* 84 (2012), pp. 487–515.

[38] Hal, R. van, Eijkel, J., and Bergveld, P. "A general model to describe the electrostatic potential at electrolyte oxide interfaces". In: *Advances in Colloid and Interface Science* 69 (1996), pp. 31 –62.

[39] Hal, R. van, Eijkel, J., and Bergveld, P. "A novel description of ISFET sensitivity with the buffer capacity and double-layer capacitance as key parameters". In: *Sensors and Actuators B: Chemical* 24 (1995), pp. 201 –205.

[40] Hammond, P. A., Ali, D., and Cumming, D. R. S. "A system-on-chip digital pH meter for use in a wireless diagnostic capsule". In: *IEEE Transactions on Biomedical Engineering* 52 (2005), pp. 687–694.

[41] He, N., Gyurcsanyi, R. E., and Lindfors, T. "Electropolymerized hydrophobic polyazulene as solid-contacts in potassium-selective electrodes". In: *Analyst* 141 (10 2016), pp. 2990–2997.

[42] Herne, T. M., and Tarlov, M. J. "Characterization of DNA Probes Immobilized on Gold Surfaces". In: *Journal of the American Chemical Society* 119 (1997), pp. 8916–8920.

[43] Hu, J., Stein, A., and Buhlmann, P. "Rational design of all-solid-state ion-selective electrodes and reference electrodes". In: *TrAC Trends in Analytical Chemistry* 76 (2016), pp. 102 –114.

[44] Hu, Y. and Georgiou, P. "A Robust ISFET pH-Measuring Front-End for Chemical Reaction Monitoring". In: *IEEE Transactions on Biomedical Circuits and Systems* 8 (2014), pp. 177–185.

[45] Huang, W., Diallo, A. K., Dailey, J. L., Besar, K., and Katz, H. E. "Electrochemical processes and mechanistic aspects of field-effect sensors for biomolecules". In: *J. Mater. Chem. C* 3 (25 2015), pp. 6445–6470.

[46] Ipatov, A., Abramova, N., Bratov, A., and Dominguez, C. "Integrated multisensor chip with sequential injection technique as a base for electronic tongue devices". In: *Sensors and Actuators B: Chemical* 131 (2008). Special Issue: Selected Papers from the 12th International Symposium on Olfaction and Electronic NosesISOEN 2007 International Symposium on Olfaction and Electronic Noses, pp. 48 –52.

[47] Ishige, Y., Shimoda, M., and Kamahori, M. "Extended-gate FET-based enzyme sensor with ferrocenyl-alkanethiol modified gold sensing electrode". In: *Biosensors and Bioelectronics* 24 (2009). Selected Papers from the Tenth World Congress on Biosensors Shangai, China, May 14-16, 2008, pp. 1096 –1102.

[48] Ishige, Y., Shimoda, M., and Kamahori, M. "Immobilization of DNA Probes onto Gold Surface and its Application to Fully Electric Detection of DNA Hybridization using Field-Effect Transistor Sensor". In: *Japanese Journal of Applied Physics* 45 (2006), p. 3776.

[49] Israelachvili, J. N. *Intermolecular and Surface Forces*. Waltham, Massachusetts, USA: Academic Press, 2011.

[50] Jakobson, C., Feinsod, M, and Nemirovsky, Y. "Low frequency noise and drift in Ion Sensitive Field Effect Transistors". In: *Sensors and Actuators B: Chemical* 68 (2000), pp. 134 –139.

[51] Jamasb, S., Collins, S., and Smith, R. L. "A physical model for drift in pH ISFETs". In: *Sensors and Actuators B: Chemical* 49 (1998), pp. 146 –155.

[52] Jananta, J. and Josowicz, M. "Conducting polymers in electronic chemical sensors". In: *Nature Materials* 2 (1 2003), pp. 19–24.

[53] Janata, J. "Graphene Bio-Field-Effect Transistor Myth". In: *ECS Solid State Letters* 1 (2012), pp. M29–M31.

[54] Janata, J. *Principles of Chemical Sensors*. 2nd ed. Springer Publishing Company, Incorporated, 2009.

[55] Jang, H.-J., Ahn, J., Kim, M.-G., Shin, Y.-B., Jeun, M., Cho, W.-J., and Lee, K. H. "Electrical signaling of enzyme-linked immunosorbent assays with an ion-sensitive field-effect transistor". In: *Biosensors and Bioelectronics* 64 (2015), pp. 318 –323.

[56] Jayant, K., Singhai, A., Cao, Y., Phelps, J. B., Lindau, M., Holowka, D. A., Baird, B. A., and Kan, E. C. "Non-Faradaic Electrochemical Detection of Exocytosis from Mast and Chromaffin Cells Using Floating-Gate MOS Transistors". In: *Scientific Reports* 5 (2015).

[57] Jayant, K., Auluck, K., Funke, M., Anwar, S., Phelps, J. B., Gordon, P. H., Rajwade, S. R., and Kan, E. C. "Programmable ion-sensitive transistor interfaces. I. Electrochemical gating". In: *Phys. Rev. E* 88 (1 2013), p. 012801.

[58] Jayant, K., Auluck, K., Funke, M., Anwar, S., Phelps, J. B., Gordon, P. H., Rajwade, S. R., and Kan, E. C. "Programmable ion-sensitive transistor interfaces. II. Biomolecular sensing and manipulation". In: *Phys. Rev. E* 88 (1 2013), p. 012802.

[59] J.F.Schenck. In: *Theory, Design, and Biomedical Applications of Solid State Chemical Sensors, ed. P.W. Cheung, CRC Press, Boca Raton.* 1978, pp. 165–173.

[60] Jiang, Z. and Stein, D. "Charge regulation in nanopore ionic field-effect transistors". In: *Phys. Rev. E* 83 (3 2011).

[61] Jiang, Z. and Stein, D. "Electrofluidic Gating of a Chemically Reactive Surface". In: *Langmuir* 26 (2010), pp. 8161–8173.

[62] Jimenez-Jorquera, C., Orozco, J., and Baldi, A. "ISFET Based Microsensors for Environmental Monitoring". In: *Sensors* 10 (2009), pp. 61–83.

[63] Kaisti, M., Zhang, Q., Prabhu, A., Lehmusvuori, A., Rahman, A., and Levon, K. "An Ion-Sensitive Floating Gate FET Model: Operating Principles and Electrofluidic Gating". In: *IEEE Transactions on Electron Devices* 62 (2015), pp. 2628–2635.

[64] Kaisti, M., Knuutila, A., Boeva, Z., Kvarnström, C., and Levon, K. "Low-Cost Chemical Sensing Platform With Organic Polymer Functionalization". In: *IEEE Electron Device Letters* 36 (2015), pp. 844–846.

[65] Kaisti, M., Zhang, Q., and Levon, K. "Compact model and design considerations of an ion-sensitive floating gate FET". In: *Sensors and Actuators B: Chemical* 241 (2017), pp. 321 –326.

[66] Kaisti, M., Boeva, Z., Koskinen, J., Nieminen, S., Bobacka, J., and Levon, K. "Hand-Held Transistor Based Electrical and Multiplexed Chemical Sensing System". In: *ACS Sensors* (2016).

[67] Kamahori, M., Ishige, Y., and Shimoda, M. "Detection of DNA hybridization and extension reactions by an extended-gate field-effect transistor: Characterizations of immobilized DNA probes and role of applying a superimposed high-frequency voltage onto a reference electrode". In: *Biosensors and Bioelectronics* 23 (2008), pp. 1046 –1054.

[68] Karnik, R., Castelino, K., and Majumdar, A. "Field-effect control of protein transport in a nanofluidic transistor circuit". In: *Applied Physics Letters* 88 (2006).

[69] Kilic, M. S., Bazant, M. Z., and Ajdari, A. "Steric effects in the dynamics of electrolytes at large applied voltages. I. Double-layer charging". In: *Phys. Rev. E* 75 (2 2007), p. 021502.

[70] Kinlen, P., Frushour, B., Ding, Y., and Menon, V. "International Conference on Science and Technology of Synthetic Synthesis and Characterization of Organically Soluble Polyaniline and Polyaniline Block Copolymers". In: *Synthetic Metals* 101 (1999), pp. 758 –761.

[71] Kirby, B. J. *Micro- and Nanoscale Fluid Mechanics: Transport in Microfluidic Devices*. Cambrigde, England: Cambridge University Press, 2010.

[72] Kounaves, S. P., Buehler, M. G., Hecht, M. H., and West, S. "Determination of Geochemistry on Mars Using an Array of Electrochemical Sensors". In: *Environmental Electrochemistry*. 2002. Chap. 17, pp. 306–319.

[73] Kulkarni, G. S. and Zhong, Z. "Detection beyond the Debye Screening Length in a High-Frequency Nanoelectronic Biosensor". In: *Nano Letters* 12 (2012), pp. 719–723.

[74] Levon, K., Rahman, A., Sai, T., and Zhao, B. *Floating gate field effect transistors for chemical and/or biological sensing*. US Patent App. 11/033,046. 2005.

[75] Liang, R., Yin, T., and Qin, W. "A simple approach for fabricating solid-contact ion-selective electrodes using nanomaterials as transducers". In: *Analytica Chimica Acta* 853 (2015), pp. 291 –296.

[76] Lindfors, T. and Ivaska, A. "pH sensitivity of polyaniline and its substituted derivatives". In: *Journal of Electroanalytical Chemistry* 531 (2002), pp. 43 –52.

[77] Liu, Y., Georgiou, P., Prodromakis, T., Constandinou, T. G., and Toumazou, C. "An Extended CMOS ISFET Model Incorporating the Physical Design Geometry and the Effects on Performance and Offset Variation". In: *IEEE Transactions on Electron Devices* 58 (2011), pp. 4414–4422.

[78] Martinoia, S. and Massobrio, G. “A behavioral macromodel of the ISFET in SPICE”. In: *Sensors and Actuators B: Chemical* 62 (2000), pp. 182 –189.

[79] Mehrabani, S., Maker, A. J., and Armani, A. M. “Hybrid Integrated Label-Free Chemical and Biological Sensors”. In: *Sensors* 14 (2014), p. 5890.

[80] Milgrew, M., Riehle, M., and Cumming, D. S. “A large transistor-based sensor array chip for direct extracellular imaging”. In: *Sensors and Actuators B: Chemical* 111 (2005). Eurosensors XVIII 2004 The 18th European Conference on Solid-State Transducers, pp. 347 –353.

[81] Mohanty, N. and Berry, V. “Graphene-Based Single-Bacterium Resolution Biodevice and DNA Transistor: Interfacing Graphene Derivatives with Nanoscale and Microscale Biocomponents”. In: *Nano Letters* 8 (2008), pp. 4469–4476.

[82] Morf, W. E. *The Principles of ion-selective electrodes and of membrane transport*. Elseview Scientific Publishing Company, 1981.

[83] Moser, N., Lande, T. S., Toumazou, C., and Georgiou, P. “ISFETs in CMOS and Emergent Trends in Instrumentation: A Review”. In: *IEEE Sensors Journal* 16 (2016), pp. 6496–6514.

[84] Mourzina, Y., Schubert, J., Zander, W., Legin, A., Vlasov, Y., Luth, H., and Schoning, M. “Development of multisensor systems based on chalcogenide thin film chemical sensors for the simultaneous multicomponent analysis of metal ions in complex solutions”. In: *Electrochimica Acta* 47 (2001), pp. 251 –258.

[85] Nakazato, K. “An Integrated ISFET Sensor Array”. In: *Sensors* 9 (2009), pp. 8831–8851.

[86] Nakazato, K. *Potentiometric, Amperometric, and Impedimetric CMOS Biosensor Array, State of the Art in Biosensors - General Aspects, Dr. Toonika Rinken (Ed.)* InTech, 2013.

[87] Nambiar, S. and Yeow, J. T. “Conductive polymer-based sensors for biomedical applications”. In: *Biosensors and Bioelectronics* 26 (2011), pp. 1825 –1832.

[88] Nemiroski, A., Christodouleas, D. C., Hennek, J. W., Kumar, A. A., Maxwell, E. J., Fernandez-Abedul, M. T., and Whitesides, G. M. “Universal mobile electrochemical detector designed for use in resource-limited applications”. In: *Proceedings of the National Academy of Sciences* 111 (2014), pp. 11984–11989.

[89] Nikkhoo, N., Gulak, P. G., and Maxwell, K. "Rapid Detection of E. coli Bacteria Using Potassium-Sensitive FETs in CMOS". In: *IEEE Transactions on Biomedical Circuits and Systems* 7 (2013), pp. 621–630.

[90] Odijk, M., Wouden, E. van der, Olthuis, W., Ferrari, M., Tolner, E., Maagdenberg, A. van den, and Berg, A. van den. "Microfabricated solid-state ion-selective electrode probe for measuring potassium in the living rodent brain: Compatibility with DC-EEG recordings to study spreading depression". In: *Sensors and Actuators B: Chemical* 207, Part B (2015), pp. 945 –953.

[91] Perumal, V. and Hashim, U. "Advances in biosensors: Principle, architecture and applications". In: *Journal of Applied Biomedicine* 12 (2014), pp. 1 –15.

[92] Poghossian, A., Cherstvy, A., Ingebrandt, S., Offenhausser, A., and Schoning, M. "Possibilities and limitations of label-free detection of DNA hybridization with field-effect-based devices". In: *Sensors and Actuators B: Chemical* 111 (2005). Eurosensors XVIII 2004 The 18th European Conference on Solid-State Transducers, pp. 470 –480.

[93] Poghossian, A. and Schöning, M. J. "Label-Free Sensing of Biomolecules with Field-Effect Devices for Clinical Applications". In: *Electroanalysis* 26 (2014), pp. 1197–1213.

[94] Privett, B. J., Shin, J. H., and Schoenfisch, M. H. "Electrochemical Sensors". In: *Analytical Chemistry* 82 (2010), pp. 4723–4741.

[95] Prodromakis, T., Liu, Y., Yang, J., Hollinghurst, D., and Toumazou, C. "A novel design approach for developing chemical sensing platforms using inexpensive technologies". In: *Biomedical Circuits and Systems Conference (BioCAS), 2011 IEEE*. 2011, pp. 369–372.

[96] Prodromakis, T., Liu, Y., and Toumazou, C. "A Low-Cost Disposable Chemical Sensing Platform Based on Discrete Components". In: *IEEE Electron Device Letters* 32 (2011), pp. 417–419.

[97] Purvis, D, Leonardova, O, Farmakovsky, D, and Cherkasov, V. "An ultrasensitive and stable potentiometric immunosensor". In: *Biosensors and Bioelectronics* 18 (2003), pp. 1385 –1390.

[98] Rothberg, J. M. and al., et. "An integrated semiconductor device enabling non-optical genome sequencing". In: *Nature* 475 (2011), pp. 348 –352.

[99] Schasfoort, R., Bergveld, P., Kooyman, R., and Greve, J. "Possibilities and limitations of direct detection of protein charges by means of an immunological field-effect transistor". In: *Analytica Chimica Acta* 238 (1990), pp. 323 –329.

[100] Schoning, M. J. and Poghossian, A. “Recent advances in biologically sensitive field-effect transistors (BioFETs)”. In: *Analyst* 127 (9 2002), pp. 1137–1151.

[101] Schoot, B. H. van der and Bergveld, P. “ISFET based enzyme sensors”. In: *Biosensors* 3 (1987), pp. 161 –186.

[102] “Sensitivity and hysteresis effect in Al2O3 gate pH-ISFET”. In: *Materials Chemistry and Physics* 71 (2001), pp. 120 –124.

[103] Shen, N. Y.-M., Liu, Z., Lee, C., Minch, B. A., and Kan, E. C.-C. “Charge-based chemical sensors: a neuromorphic approach with chemoreceptive neuron MOS (CνMOS) transistors”. In: *IEEE Transactions on Electron Devices* 50 (2003), pp. 2171–2178.

[104] Shepherd, L. M. and Toumazou, C. “A biochemical translinear principle with weak inversion ISFETs”. In: *IEEE Transactions on Circuits and Systems I: Regular Papers* 52 (2005), pp. 2614–2619.

[105] Souteyrand, E., Cloarec, J. P., Martin, J. R., Wilson, C., Lawrence, I., Mikkelsen, S., and Lawrence, M. F. “Direct Detection of the Hybridization of Synthetic Homo-Oligomer DNA Sequences by Field Effect”. In: *The Journal of Physical Chemistry B* 101 (1997), pp. 2980–2985.

[106] spiegel, J. van der, Lauks, I., Chan, P., and Babic, D. “The extended gate chemically sensitive field effect transistor as multi-species microprobe”. In: *Sensors and Actuators* 4 (1983), pp. 291 –298.

[107] Squires, T. M., Messinger, R. J., and Manalis, S. R. “Making it stick: convection, reaction and diffusion in surface-based biosensors”. In: *Nat Biotech* 26 (2008), pp. 417 –426.

[108] Stein, D., Kruithof, M., and Dekker, C. “Surface-Charge-Governed Ion Transport in Nanofluidic Channels”. In: *Phys. Rev. Lett.* 93 (3 2004).

[109] Streetman, B. G. and Banerjee, S. K. *Solid State Electronic Devices*. New Jersey, USA: Pearson Prentice Hall, 2006.

[110] Tarasov, A., Gray, D. W., Tsai, M.-Y., Shields, N., Montrose, A., Creedon, N., Lovera, P., O’Riordan, A., Mooney, M. H., and Vogel, E. M. “A potentiometric biosensor for rapid on-site disease diagnostics”. In: *Biosensors and Bioelectronics* 79 (2016), pp. 669 –678.

[111] Toumazou, C. and al., et. “Simultaneous DNA amplification and detection using a pH-sensing semiconductor system”. In: *Nature Methods* 10 (2013), pp. 641 –646.

[112] Uslu, F., Ingebrandt, S., Mayer, D., Bocker-Meffert, S., Odenthal, M., and Offenhausser, A. "Labelfree fully electronic nucleic acid detection system based on a field-effect transistor device". In: *Biosensors and Bioelectronics* 19 (2004), pp. 1723 –1731.

[113] Vanamo, U. "Solid-State Reference and Ion-Selective Electrodes - Towards Portable Potentiometric Sensing". PhD thesis. Åbo Academi, 2013.

[114] Velde, L. van de, d'Angremont, E., and Olthuis, W. "Solid contact potassium selective electrodes for biomedical applications a review". In: *Talanta* 160 (2016), pp. 56 –65.

[115] Vieira, N. C., Fernandes, E. G., Faceto, A. D., Zucolotto, V., and Guimaraes, F. E. "Nanostructured polyaniline thin films as pH sensing membranes in FET-based devices". In: *Sens. Actuators, B* 160 (2011), pp. 312 –317.

[116] Walsh, K. B., DeRoller, N., Zhu, Y., and Koley, G. "Application of ion-sensitive field effect transistors for ion channel screening". In: *Biosensors and Bioelectronics* 54 (2014), pp. 448 –454.

[117] Wan, Y., Su, Y., Zhu, X., Liu, G., and Fan, C. "Development of electrochemical immunosensors towards point of care diagnostics". In: *Biosensors and Bioelectronics* 47 (2013), pp. 1 –11.

[118] Xu, G., Abbott, J., Qin, L., Yeung, K. Y. M., Song, Y., Yoon, H., Kong, J., and Ham, D. "Electrophoretic and field-effect graphene for all-electrical DNA array technology". In: *Nat Commun* 5 (2015).

[119] Yeow, T., Haskard, M., Mulcahy, D., Seo, H., and Kwon, D. "A very large integrated pH-ISFET sensor array chip compatible with standard CMOS processes". In: *Sensors and Actuators B: Chemical* 44 (1997), pp. 434 –440.

[120] Zeng, X., Yu, S., Yuan, Q., and Qin, W. "Solid-contact K+-selective electrode based on three-dimensional molybdenum sulfide nanoflowers as ion-to-electron transducer". In: *Sensors and Actuators B: Chemical* 234 (2016), pp. 80 –83.

[121] Zhang, G.-J. and Ning, Y. "Silicon nanowire biosensor and its applications in disease diagnostics: A review". In: *Analytica Chimica Acta* 749 (2012), pp. 1 –15.

[122] Zhang, Q., Majumdar, H. S., Kaisti, M., Prabhu, A., Ivaska, A., Österbacka, R., Rahman, A., and Levon, K. "Surface Functionalization of Ion-Sensitive Floating-Gate Field-Effect Transistors With Organic Electronics". In: *IEEE Transactions on Electron Devices* 62 (2015), pp. 1291–1298.

[123] Zhang, Q. "Oligomeric and polymeric aniline based organic electronics and their applications in charge modulated electrochemical biosensing devices". PhD thesis. New Youk University Polytechnic School of Engineering, 2014.

[124] Zhang, Q., Prabhu, A., San, A., Al-Sharab, J. F., and Levon, K. "A polyaniline based ultrasensitive potentiometric immunosensor for cardiac troponin complex detection". In: *Biosensors and Bioelectronics* 72 (2015), pp. 100 –106.

[125] Zhang, X., Ju, H., and Wang, J. *Electrochemical Sensors, Biosensors and Their Biomedical Applications*. Academic Press, 2008.

[126] Zhu, C., Yang, G., Li, H., Du, D., and Lin, Y. "Electrochemical Sensors and Biosensors Based on Nanomaterials and Nanostructures". In: *Analytical Chemistry* 87 (2015), pp. 230–249.